The University of Sydney
Department of Civil Engineering
Sydney NSW 2006
AUSTRALIA

http://www.civil.usyd.edu.au/

Centre for Advanced Structural Engineering

Full-range Stress-strain Curves for Stainless Steel Alloys

Research Report No R811

By

Kim JR Rasmussen MScEng, PhD

November 2001

The University of Sydney

Department of Civil Engineering
Centre for Advanced Structural Engineering
http://www.civil.usyd.edu.au

Full-range Stress-strain Curves for Stainless Steel Alloys

Research Report No R811

Kim JR Rasmussen, MScEng, PhD

November 2001

Abstract:

The report develops an expression for the stress-strain curves for stainless steel alloys which is valid over the full strain range. The expression is useful for the design and numerical modelling of stainless steel members and elements which reach stresses beyond the 0.2% proof stress in their ultimate limit state. In this stress range, current stress-strain curves based on the Ramberg-Osgood expression become seriously inaccurate principally because they are extrapolations of curve fits to stresses lower than the 0.2% proof stress. The extrapolation becomes particularly inaccurate for alloys with pronounced strain hardening.

The report also develops expressions for determining the ultimate tensile strength (σ_u) and strain (ε_u) for given values of the Ramberg-Osgood parameters (E_0,$\sigma_{0.2}$,n). The expressions are compared with a wide range of experimental data and shown to be reasonably accurate for all structural classes of stainless steel alloys. Based on the expressions for (σ_u) and (ε_u), it is possible to construct the entire stress-strain curve from the Ramberg-Osgood parameters (E_0,$\sigma_{0.2}$,n).

Keywords:

Stainless steel, stress-strain curves, Ramberg-Osgood curve, tests.

Copyright Notice

Department of Civil Engineering, Research Report R811
Full-range Stress-strain Curves for Stainless Steel Alloys

k.rasmussen@civil.usyd.edu.au

Published by:
Department of Civil Engineering
The University of Sydney
Sydney, NSW, 2006
AUSTRALIA

November 2001

http://www.civil.usyd.edu.au

Introduction

Stainless steel alloys have low proportionality limits and extended strain-hardening capability. The pronounced yield plateau familiar from structural steel is nonexistent and so an equivalent yield stress is used in structural design, usually chosen as a suitable proof stress. The nonlinear stress-strain behaviour is acknowledged in the American (ASCE, 1991), Australian (AS/NZS 4673, 2001) and South African (SABS 1997) standards for cold-formed stainless steel structures which define the stress-strain curve in terms of the Ramberg-Osgood expression (Ramberg and Osgood, 1941),

$$\varepsilon = \frac{\sigma}{E_0} + p\left(\frac{\sigma}{\sigma_p}\right)^n. \tag{1}$$

Equation 1 was originally developed for aluminium alloys but has proven suitable for other nonlinear metals including stainless steel alloys. It involves the initial Young's modulus (E_0), the proof stress (σ_p) corresponding to the plastic strain p, and a parameter (n) which determines the sharpness of the knee of the stress-strain curve. In the design of aluminium and stainless steel structures, it has become industry practice to use the 0.2% proof stress ($\sigma_{0.2}$) as the equivalent yield stress. For this proof stress, the stress-strain relationship takes the form,

$$\varepsilon = \frac{\sigma}{E_0} + 0.002\left(\frac{\sigma}{\sigma_{0.2}}\right)^n. \tag{2}$$

It has also become standard practice to determine the parameter (n) using the 0.01% and 0.2% proof stresses which leads to the following expression,

$$n = \frac{\ln(20)}{\ln(\sigma_{0.2}/\sigma_{0.01})}. \tag{3}$$

Equation 3 ensures that the Ramberg-Osgood approximation matches exactly the measured stress-strain curve at the 0.01% and 0.2% proof stresses. It generally provides close approximations to measured stress-strain curves for stresses *up to* the 0.2% proof stress.

In concentrically loaded columns, the strains are small when reaching the ultimate load for all practical ranges of length. It is therefore possible to base the design on the Ramberg-Osgood curve and achieve close agreement with experimental strengths, e.g. see Rasmussen and Hancock (1993) and Rhodes et al. (2000). Rasmussen and Rondal (1997) used this result to develop a direct relationship between the column strength and the parameters n and e, where e is the nondimensional proof stress,

$$e = \frac{\sigma_{0.2}}{E_0}. \tag{4}$$

However, structural components which undergo significant straining before reaching their ultimate capacity, such as plates in compression or shear, compact beams failing by in-plane bending and tension members, may develop stresses beyond the 0.2% proof stress and strains well in excess of the 0.2% total strain,

$$\varepsilon_{0.2} = \frac{\sigma_{0.2}}{E_0} + 0.002. \tag{5}$$

When the strains exceed the 0.2% total strain ($\varepsilon_{0.2}$), the Ramberg-Osgood curve obtained on the basis of the 0.01% and 0.2% proof stresses may become seriously inaccurate, tending to

produce too high stresses, as shown in Fig. 1. This particularly applies to alloys with low values of *n*. In this strain range, it is necessary to use a refined expression for the stress-strain curve with wider applicability range. This report aims to develop such an expression within the following constraints:

1. Current values of *n*, such as those given in the American, Australian and South African standards for stainless steel structures, shall remain applicable. This implies that the stress-strain curve can be accurately determined using the Ramberg-Osgood expression for stresses up to the 0.2% proof stress.
2. In the stress range between the 0.2% proof stress and the ultimate tensile strength (σ_u), the stress-strain curve shall be defined in terms of a *minimum* of additional parameters.

These constraints ensure simplicity in the stress-strain curve formulation. It will be demonstrated that it is possible to obtain agreement with measured stress-strain curves within tolerances that would be deemed acceptable for a wide range of applications.

Recent approaches

MacDonald et al. (2000) reported a series of tests on austenitic UNS30400 (AISI304) stainless steel channel columns. Ramberg-Osgood curves were fitted to stress-strain curves obtained from stub column and tension coupon testing by using the 0.01% and 0.2% proof stresses to determine the *n*-parameter. The fitted Ramberg-Osgood curves were shown to err significantly at strains exceeding the 0.2% total strain ($\varepsilon_{0.2}$) and a modified expression was suggested in the form

$$\varepsilon = \frac{\sigma}{E_0} + 0.002\left(\frac{\sigma}{\sigma_1}\right)^{\left(i+j\left(\frac{\sigma}{\sigma_1}\right)^k\right)} \tag{6}$$

where the constants i, j and k took values ranging from 2.5 to 6 depending on the thickness of the material tested. While this expression proved very accurate, it was limited in applicability to the particular alloy and thicknesses tested.

Olsson (2001) studied advanced plasticity models for stainless steel alloys and performed a large number of tests on uniaxially and biaxially loaded coupons. He plotted the stress-strain curves as true stress (σ^t) *vs* engineering strain (ε) and observed experimentally that the stress-strain curve approached a straight line at large strains. He proposed that the true-stress *vs* engineering strain curve be approximated by a Ramberg-Osgood curve for strains up to a total strain of 2% and a straight line from this point onwards, as shown in Fig. 2. The straight line was chosen as an average fit to the measured stress-strain curve. It was not required to equal the true ultimate tensile strength (σ^t_u) at the ultimate total strain (ε_u).

Acknowledging the relationship between the true and engineering stresses,

$$\sigma^t = \sigma(1+\varepsilon) \tag{7}$$

and observing that $d\sigma/d\varepsilon \to 0$ for $\sigma \to \sigma_u$, it is apparent that as $\sigma \to \sigma_u$ the true stress *vs* engineering strain curve asymptotes to the line,

$$\sigma^t = \sigma_u(1+\varepsilon). \tag{8}$$

Evidently, the slope of this line and the intercept of the line with the stress axis both equal σ_u, as shown in Fig. 2. The slope of the line is different from the slope of the line through the true 2% proof stress and true ultimate tensile strength.

While Olsson's approach is attractive because of its theoretical justification, it lacks accuracy at small strains since it assumes the Ramberg-Osgood curve is valid for total strains up to 2%. Olsson determined the *n*-parameter by use of the 0.2% and 1% proof stresses which implies compromised accuracy in the important strain range $\varepsilon<\varepsilon_{0.2}$. In view of Constraint #1 stated in the Introduction, Olsson's approach has not been adopted in this report. However, it may prove appropriate for applications concerned mainly with large strains.

Test data

A wide range of tests has been used to develop the full-range stress-strain relation, including coupon tests on austenitic, duplex and ferritic stainless steel alloys. To cover the practical range of proof stress and *n*-values, the test data includes coupons cut from annealed plate as well as cold-formed sections (rectangular hollow sections (RHS), circular hollow sections (CHS) and channels sections). The data is summarised in Table 1. Thirteen tests were performed on austenitic alloys (UNS30400, UNS30403, UNS31603), four on duplex alloys (UNS31803), and two on ferritic alloys (UNS43000, 3Cr12). The values of *n* range from 4.45 to 12.2, as shown in Table 1. The values of nondimensional proof stress ($e=\sigma_{0.2}/E_0$) range from 0.0014 to 0.0037.

Several references used for the experimental data did not include values of initial modulus (E_0) or proportionality stress ($\sigma_{0.01}$). In these cases, the values were determined from the stress-strain curves. In cases where the *n*-parameter was not presented, the value was calculated using Eqn. 3.

Stress-strain curve expression

In view of Constraint #1 mentioned in the Introduction, the stress-strain curve is chosen as a standard Ramberg-Osgood curve for stresses up to the 0.2% proof stress,

$$\varepsilon = \frac{\sigma}{E_0} + 0.002\left(\frac{\sigma}{\sigma_{0.2}}\right)^n \quad \text{for } \sigma \le \sigma_{0.2}. \tag{9}$$

In developing a model for the part of the stress-strain curve between the 0.2% proof stress and the ultimate tensile strength (σ_u), it is noted that the stress-strain curve in this range is similar in shape to the initial part of the stress-strain curve up to the 0.2% proof stress, as shown in Fig. 3.

This observation suggests a linear transformation of the stress and strain and the use of the Ramberg-Osgood expression (Eqn. 1) in the following form,

$$\bar{\varepsilon} = \frac{\bar{\sigma}}{E_{0.2}} + \varepsilon_{u_p}\left(\frac{\bar{\sigma}}{\bar{\sigma}_u}\right)^m \quad \text{for } \sigma > \sigma_{0.2} \tag{10}$$

where $\bar{\varepsilon}$ and $\bar{\sigma}$ are the transformed strain and stress (see Fig. 3b), defined as

$$\bar{\varepsilon} = \varepsilon - \varepsilon_{0.2} \tag{11}$$

$$\bar{\sigma} = \sigma - \sigma_{0.2}\ . \tag{12}$$

The initial modulus to the curve ($E_{0.2}$) is also the tangent modulus of the stress-strain curve at the 0.2% proof stress, as shown in Fig. 3. By requiring continuity in slope at $\sigma_{0.2}$, $E_{0.2}$ is obtained from Eqn. 9 as $d\sigma / d\varepsilon\big|_{\sigma=\sigma_{0.2}}$,

$$E_{0.2} = \frac{E_0}{1 + 0.002n/e}. \tag{13}$$

In adopting Eqn. 1, the "proof stress" (σ_p) is taken as the transformed ultimate tensile strength ($\overline{\sigma}_u$),

$$\overline{\sigma}_u = \sigma_u - \sigma_{0.2} \tag{14}$$

and accordingly, the plastic strain (p) is the transformed ultimate plastic strain ($\overline{\varepsilon}_{u_p}$),

$$\overline{\varepsilon}_{u_p} = \varepsilon_u - \varepsilon_{0.2} - \sigma_u / E_0. \tag{15}$$

Stainless steel alloys are generally ductile and so negligible error is made by approximating the transformed ultimate plastic strain by the total ultimate strain,

$$\overline{\varepsilon}_{u_p} \approx \varepsilon_u. \tag{16}$$

The exponent (m) is obtained by trial and error using the stress-strain curves reported in the references summarised in note (b) of Table 1. Recognising that the exponent is dependent on the ultimate tensile strength in relation to the 0.2% proof stress, the following expression was obtained,

$$m = 1 + 3.5\frac{\sigma_{0.2}}{\sigma_u}. \tag{17}$$

The full-range stress-strain curve can be written out in full as follows:

$$\varepsilon = \begin{cases} \dfrac{\sigma}{E_0} + 0.002\left(\dfrac{\sigma}{\sigma_{0.2}}\right)^n & \text{for } \sigma \le \sigma_{0.2} \\ \dfrac{\sigma - \sigma_{0.2}}{E_{0.2}} + \varepsilon_u\left(\dfrac{\sigma - \sigma_{0.2}}{\sigma_u - \sigma_{0.2}}\right)^m + \varepsilon_{0.2} & \text{for } \sigma > \sigma_{0.2} \end{cases} \tag{18}$$

where $E_{0.2}$ and m are given by Eqns 13 and 17 respectively. Figures 4, 5 and 6 show typical comparisons of the stress-stain curves obtained using Eqn. 18 with experimental data for austenitic, duplex and ferritic alloys respectively. The complete set of curves for the 19 tests listed in Table 1 are contained in Appendix A.

The agreement between the test and proposed full-range stress-strain curves is generally excellent, while the Ramberg-Osgood curves extended past the 0.2% proof stress become increasingly inaccurate with strain, as shown in Figs 4-6. The agreement is particularly good for the UNS30403 alloy, as shown in Fig. 4. The coupon test on UNS40300 alloy conducted by Korvink and van den Berg (1993) was only reported for strains up to 0.007, as shown in Fig. 6. The agreement is good in this strain range. The agreement for the (duplex) UNS31803 is reasonable although the proposed curve is higher than the test curve immediately after the 0.2% proof stress, as shown in Fig. 5. The discrepancy is a consequence of the slope ($E_{0.2}$) of the Ramberg-Osgood curve determined at the 0.2% proof stress which is too high.

Expressions for ε_u and σ_u

The expression for the full-range stress-strain curve (Eqn. 18) involves three parameters (E_0,n,$\sigma_{0.2}$) for $\sigma \le \sigma_{0.2}$ and two additional parameters (ε_u,σ_u) for $\sigma > \sigma_{0.2}$. In many situations, the values of ε_u and σ_u may not be available or may not be achievable experimentally, as in the testing of compression coupons. To cater for these situations, equations are developed in this section for the determination of ε_u and σ_u in terms of n and e, where e is the nondimensional equivalent yield stress given by Eqn. 4.

The experimental data is that contained in Table 1 augmented by the results given in a report by the Steel Construction Institute (SCI, 1991) and reports by the Rand African University (van der Merwe et al. 1986, van der Merwe and van den Berg 1987). These reports do not contain complete stress-strain curves and could not be used for deriving a full-range expression for the stress-strain curves, as described in Section 4. The SCI report details 227 tension and compression coupon tests on austenitic (UNS30403, UNS31603) and duplex (UNS31803) alloys, while the South African reports detail tension and compression tests on ferritic UNS40300 stainless steel and weldable 12% chromium containing corrosion resisting steel, popularly know as 3Cr12, which is closely related to the ferritic alloy class. 288 tests are contained in the South African reports for various thicknesses and direction of loading (longitudinal and transverse). Only the mean values of the results for each alloy, thickness and direction of loading have been used in this report, adding a further 12 "tests" to the database. The British and South African experimental data is summarised in Appendix B.

Evidently, the 0.2% proof stress approaches the ultimate tensile strength when increased by cold-forming, as is commonly found in austenitic alloys. This suggests that a relationship may exist between the ratio $\sigma_{0.2}/\sigma_u$ and the 0.2% proof stress. Accordingly, the ratio $(\sigma_{0.2}/\sigma_u)$ is plotted against the nondimensional proof stress (e), as shown in Fig. 7. The graph indicates a linear relationship when excluding the ferritic alloys. A line of best fit through the test data for austenitic and duplex alloys produces the following equation,

$$\frac{\sigma_{0.2}}{\sigma_u} = 0.2 + 185e \quad \text{(austenitic and duplex alloys).} \tag{19}$$

The ferritic alloys (including 3Cr12) generally have larger n-values than austenitic and duplex alloys. Hence, their stress-strain curves have sharper knees which explain the higher values of $(\sigma_{0.2}/\sigma_u)$ for given value of e, as shown in Fig. 7. To account for the influence of n, the following expression for $\sigma_{0.2}/\sigma_u$ has been obtained,

$$\frac{\sigma_{0.2}}{\sigma_u} = \frac{0.2 + 185e}{1 - 0.0375(n-5)} \quad \text{(all alloys).} \tag{20}$$

Figure 8 shows the experimental values of $(\sigma_{0.2}/\sigma_u)$ plotted against the approximate values given by Eqn. 20. The data points are shown with solid markers and are not biased towards a particular alloy. However, they have greater scatter compared to the data points based on Eqn. 19 which are shown with open markers in Fig. 8. Equation 20 is therefore less accurate than Eqn. 19 for austenitic and duplex alloys but is more generally applicable.

Finally, an expression is sought for determining the ultimate tensile total strain (ε_u). Recognising that $\varepsilon_u \to 0$ for $\sigma_{0.2} \to \sigma_u$, the ultimate tensile strain is plotted against the ratio of 0.2% proof stress to ultimate tensile strength, as shown in Fig. 9.

There is significant scatter in the plot, as could be expected given the generally large variability in values of ultimate tensile strain. It is also not clear whether the ultimate tensile strain quoted in the references were the uniform elongation at the ultimate tensile strength, as has been assumed, or the total strain after fracture including local elongation in the area of necking.

The line of best fit can be closely approximated by,

$$\varepsilon_u = 1 - \frac{\sigma_{0.2}}{\sigma_u}. \tag{21}$$

as shown with a solid line in Fig. 9. The data points are not biased towards a particular alloy and no attempt has been made to explore a possible relationship between ε_u and the n-parameter.

With Eqns 20 and 21 at hand for determining σ_u and ε_u, the full-range stress-strain curves can be obtained from Eqn. 18 for given values of E_0, $\sigma_{0.2}$ and n.

To assess the effect of the variability associated with Eqns 20 and 21, stress-strain curves have been determined for the combinations of σ_u and ε_u shown in Tables 2 and 3 respectively. In all cases, the Ramberg-Osgood parameters were taken as (E_0=200 GPa, $\sigma_{0.2}$=400 MPa, n=6), and the reference values of (σ_u=675 MPa, ε_u=0.408) were determined using Eqns (20,21). In Table 2, the ultimate tensile strength (σ_u) is changed by ±10% and ±20% while keeping ε_u=0.408 constant. Conversely, in Table 3, the ultimate tensile strain (ε_u) is changed by ±20% and ±40% while keeping σ_u=675MPa constant. These changes in ultimate tensile strength and strain are representative of the largest differences between test data and the values of σ_u and ε_u determined using Eqns 19 and 20 respectively, as shown in Figs 8 and 9. The stress-strain curves resulting from the values of σ_u and ε_u given in Tables 2 and 3 are shown in Figs 10 and 11 respectively.

The changes in stress at a strain of 2% are shown in the 4th columns of Tables 2 and 3. It follows from Table 2 that for the chosen values of (E_0,$\sigma_{0.2}$,n), a reduction of 20% in σ_u leads to a 7.1% decrease in $\sigma(\varepsilon=2\%)$. According to Table 3, a reduction of 40% in ε_u leads to a 2.7% increase in $\sigma(\varepsilon=2\%)$. Since these deviations in σ_u and ε_u represent the maximum deviations of the test data, it can be concluded that the expressions given by Eqns 20 and 21 are likely to produce stress-strain curves with a maximum error of about 7% in stress at a strain of 2%, which for many applications is a likely upper bound to the ultimate limit state strains.

Conclusions

An expression has been derived (Eqn. 18) for the complete stress-strain curve for stainless steel alloys. The expression involves the conventional Ramberg-Osgood parameters (E_0, $\sigma_{0.2}$, n) as well as the ultimate tensile strength (σ_u) and strain (ε_u). It has been shown to produce stress-strain curves which are in good agreement with tests over the full range of strains up to the ultimate tensile strain.

Expressions are also derived for the ultimate tensile strength (σ_u) and strain (ε_u) in terms of the Ramberg-Osgood parameters, see Eqns 20 and 21. The expressions are generally in reasonable agreement with experimental data. The maximum deviations observed are of the order of 20% for the ultimate tensile strength (σ_u) and 40% for the ultimate tensile strain (ε_u). It is shown that a deviation in σ_u of 20% produces a maximum error in stress of 7.1% at a strain of 2% for a typical stainless steel alloy. Likewise, a deviation in ε_u of 40% produces a maximum error in stress of 2.7% at a strain of 2%. It can be concluded that the maximum variability associated with using Eqns 20 and 21 leads to a maximum error on the stress of the order of 7% at a strain of 2%.

By using Eqns 20 and 21 to determine (σ_u) and (ε_u), the full-range stress-strain curve can be obtained directly from the Ramberg-Osgood parameters (E_0, $\sigma_{0.2}$, n). This result is particularly useful for the design and numerical modelling of stainless steel structural members and elements where the stress-strain curve is specified in terms of the Ramberg-Osgood parameters, such as in the Australian, American and South African specifications for stainless steel structures.

References

ASCE, (1991), *Specification for Cold-formed Stainless Steel Structural Members*, ANSI/ASCE-8, American Society of Civil Engineers, New York.

AS/NZS4673, (2001), *Cold-formed Stainless Steel Structures*, Standards Australia, Sydney.

Burns, T and Bezkorovainy, P, (2001), *Buckling of Stiffened Stainless Steel Plates*, BE (Honours) Thesis, Department of Civil Engineering, University of Sydney.

Korvink, SA and van den Berg, GJ, (1993), "Web Crippling of Stainless Steel Cold-formed Beams", *Proceedings*, SSRC Annual Technical Session.

MacDonald, M, Rhodes, J and Taylor, GT, (2000), "Mechanical Properties of Stainless Steel Lipped Channels", *Proceedings*, 15th International Specialty Conference on Cold-formed Steel Structures. Eds RA LaBoube and W-W Yu, University of Missouri-Rolla, p. 673-686.

Olsson, A., (2001), *Stainless Steel Plasticity – Material Modelling and Structural Applications*, PhD thesis, Department of Civil and Mining Engineering, Luleå University of Technology, Sweden.

Ramberg, W and Osgood, WR, (1941), "Determination of Stress-strain Curves by Three Parameters", Technical Note No. 503, National Advisory Committee on Aeronautics, (NACA).

Rasmussen, KJR and Hancock, GJ, (1993), "Design of Cold-formed Stainless Steel Tubular Members. I: Columns", *Journal of Structural Engineering,* ASCE, **119**(8), p. 2349-2367.

Rasmussen, KJR and Rondal, J, (1997), "Strength Curves for Metal Columns", *Journal of Structural Engineering*, ASCE, **123**(6), p. 721-728.

Rhodes, J, MacDonald, M and McNiff, W, (2000), "Buckling of Stainless Steel Columns under Concentric and Eccentric Loading", *Proceedings*, 15th International Specialty Conference on Cold-formed Steel Structures. Eds RA LaBoube and W-W Yu, University of Missouri-Rolla, p. 687-699.

SABS, (1997), *Structural Use of Steel. Part 4: The Design of Cold-formed Stainless Steel Structural Members*, The South African Bureau of Standards, Pretoria.

SCI, (1991), "Tests on Stainless Steel Materials", *Report No. SCI-RT-251*, Steel Construction Institute, London.

Talja, A and Salmi, P, (1995), "Design of Stainless Steel RHS Beams, Columns and Beam-columns", *VTT Research Note 1619*, Technical Research Centre of Finland, Espoo.

Van der Merwe, P, van den Berg, GJ, and Marshall, V, (1986), "Experimental Stress-strain Curves for Cold-rolled 3Cr12 Steel Sheets", *Internal Report No. MD-21*, Department of Civil Engineering, Rand Afrikaans University, July.

Van der Merwe, P, and van den Berg, GJ, (1987), "Experimental Stress-strain Curves for Cold-rolled Type 430 Steel Sheets", *Internal Report No. MD-36*, Department of Civil Engineering, Rand Afrikaans University, August.

Test	Alloy[a]	Source[b]	Form[c]	E_0 GPa	$\sigma_{0.01}$ MPa	$\sigma_{0.2}$ MPa	σ_u MPa	ε_u	e	n	m[f]
1	UNS30400	1	RHS	188	314	612	780	0.40	0.0032	4.49	3.7
2	UNS30400	1	RHS	182	297	532	731	0.45	0.0029	5.14	3.5
3	UNS30400	1	RHS	190	178	312	635	0.65	0.0016	5.33	2.7
4	UNS30400	1	RHS	197	183	286	627	0.65	0.0015	6.71	2.6
5	UNS30400	1	RHS	190	241	402	661	0.55	0.0021	5.85	3.1
6	UNS30400	1	RHS	196	203	297	638	0.61	0.0015	7.87	2.6
7	UNS30400	2	Ch	180	241	460	695	0.34[e]	0.0026	4.66	3.3
8	UNS30400	3	P	190	215	327	611	0.57	0.0017	7.0	2.9
9	UNS30403	4	RHS	194	240	445	730[g]	0.51[g]	0.0023	4.85	3.1
10	UNS30403	4	RHS	190	240	470	730	0.51	0.0025	4.45	3.3
11	UNS30403	4	CHS	198	250	400	675[g]	0.51[g]	0.0020	6.37	3.1
12	UNS30403	4	CHS	198	250	400	675	0.51	0.0020	6.37	3.1
13	UNS31603	3	P	190	190	316	616	0.51	0.0017	5.88	2.8
14	UNS31803	3	P	190	526	699	878	0.32	0.0037	10.6	3.8
15	UNS31803	5	P	200	310	575	805	0.22	0.0029	4.85	3.5
16	UNS31803	5	P	215	430	635	820	0.22	0.0029	7.68	3.7
17	UNS31803	5	P	215	430	635	820	0.22	0.0029	7.68	3.7
18	UNS43000	6	P	200	200	320	622[d]	0.48[e]	0.0016	6.37	2.8
19	3Cr12	6	P	195	215	275	444[d]	0.38[e]	0.0014	12.2	3.2

a) UNS30400 ~ AISI304 ~ ENV1.4301; UNS30403 ~ AISI304L ~ ENV1.4306; UNS31603 ~ AISI316L ~ ENV1.4436; UNS31803~ ENV1.4462 ~ Duplex 2205; UNS43000 ~ AISI430 ~ ENV1.4016; UNS41050 ~ 3Cr12 ~ ENV1.4003

b) 1 ~ Talja & Salmi (1995); 2 ~ McDonald et al. (2000); 3 ~ Olsson (2001); 4 ~ Rasmussen & Hancock (1993); 5 ~ Burns & Bezkorovainy (2001); 6 ~ Korvink & van den Berg (1993)

c) RHS ~ rectangular hollow section; CHS ~ circular hollow section; Ch ~ channel section; P~ plate or sheet

d) Ultimate tensile strength estimated using Eqn. 20.

e) Ultimate total strain estimated using Eqn. 21.

f) The parameter m is obtained using Eqn. 17.

g) Compression test. The values of σ_u and ε_u are assumed equal to the values for the corresponding tensile tests.

Table 1. Mechanical properties

σ_u (MPa)	% change in σ_u	$\sigma(\varepsilon=2\%)$ (MPa)	% change in $\sigma(\varepsilon=2\%)$
810	+20	513	+4.8
743	+10	502	+2.6
675	–	490	–
608	-10	474	-3.2
540	-20	455	-7.1

ε_u=0.408, E_0=200 GPa, $\sigma_{0.2}$=400 MPa, n=6

Table 2: Effect of change in σ_u

ε_u	% change in ε_u	$\sigma(\varepsilon=2\%)$ (MPa)	% change in $\sigma(\varepsilon=2\%)$
0.571	+40	481	-1.8
0.490	+20	485	-1.0
0.408	–	490	–
0.326	-20	496	+1.3
0.255	-40	502	+2.7

σ_u=675 MPa, E_0=200 GPa, $\sigma_{0.2}$=400 MPa, n=6

Table 3: Effect of change in ε_u

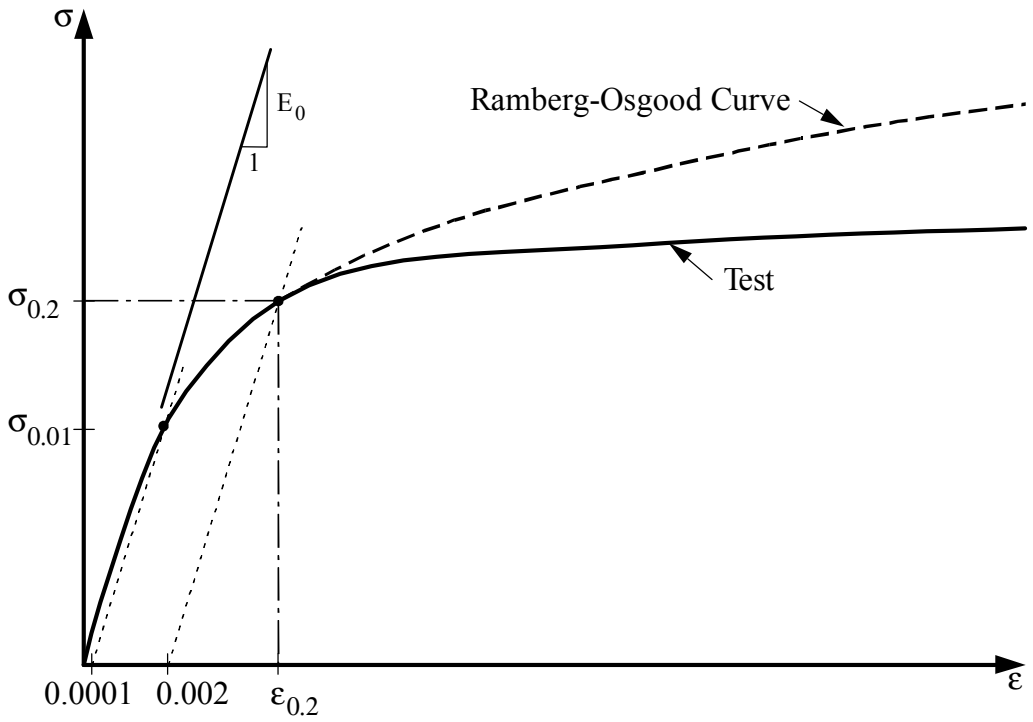

Figure 1. Typical stress-strain curve for stainless steel and Ramberg-Osgood approximation.

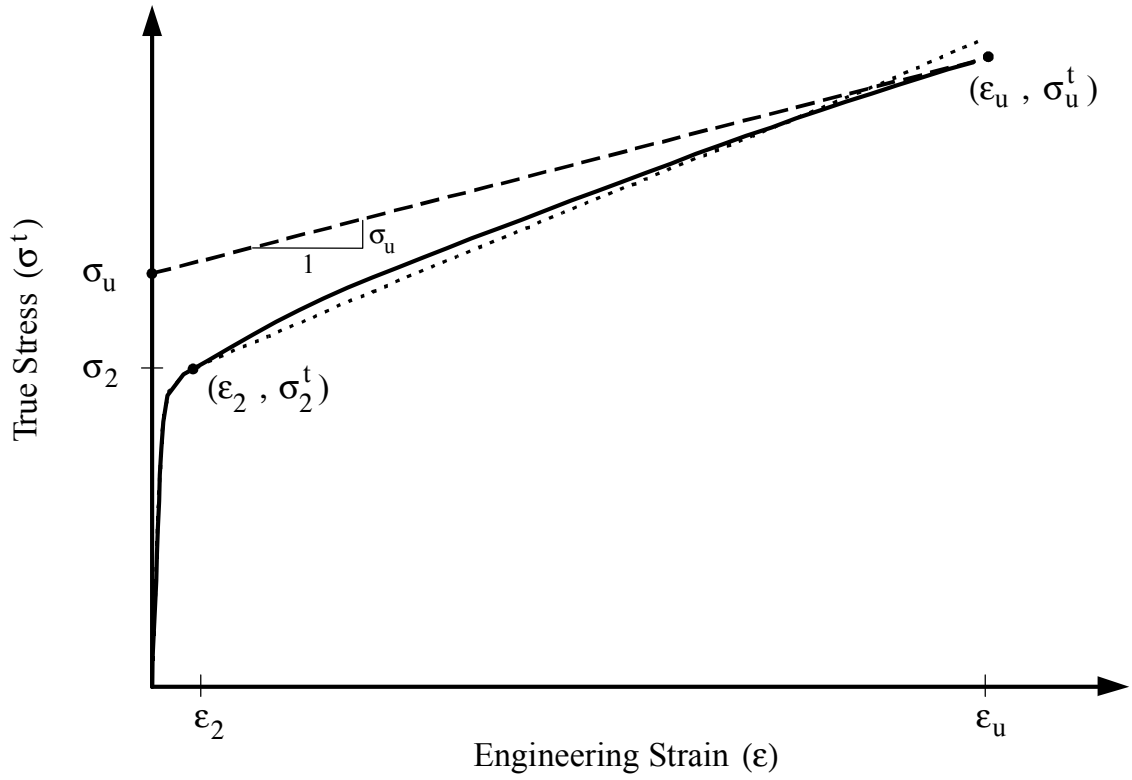

Figure 2. Stress-strain curve in terms of true stress, and comparison with Olsson's model.

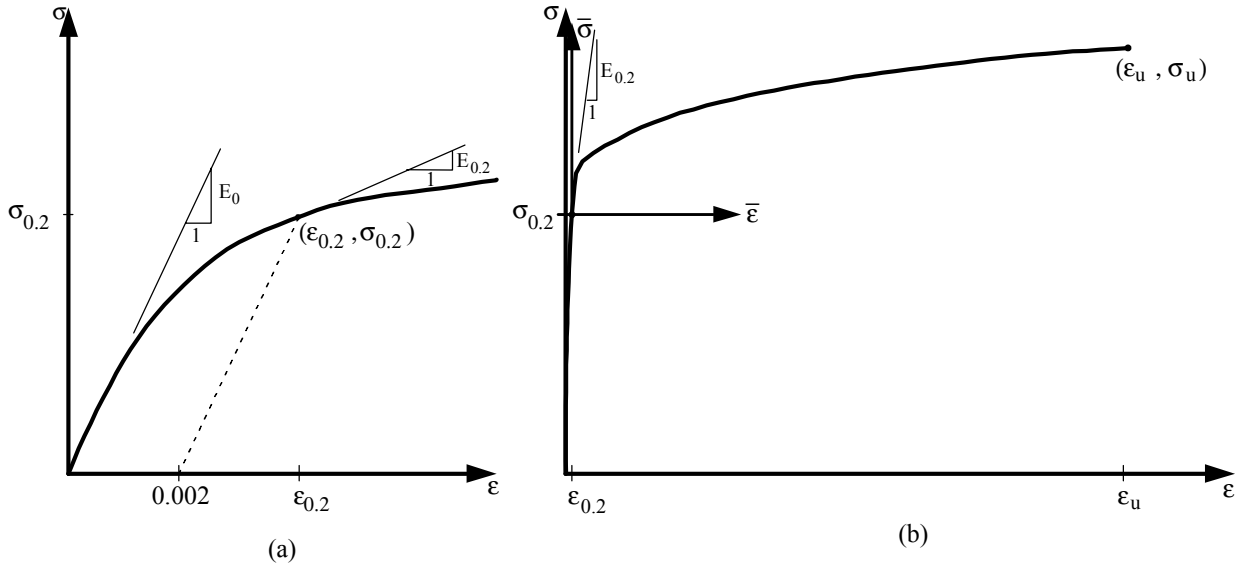

a) initial σ-ε curve b) full σ-ε curve

Figure 3. Initial and full stress-strain curves.

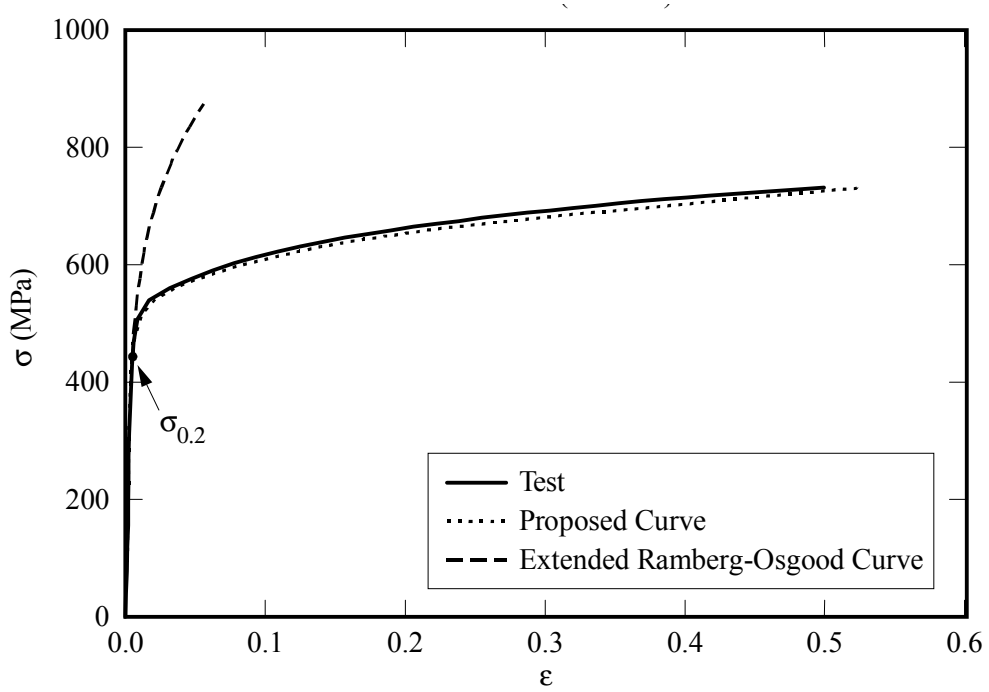

Figure 4. Stress-strain curves for UNS30403 alloy. Test #9, see Table 1 for source.

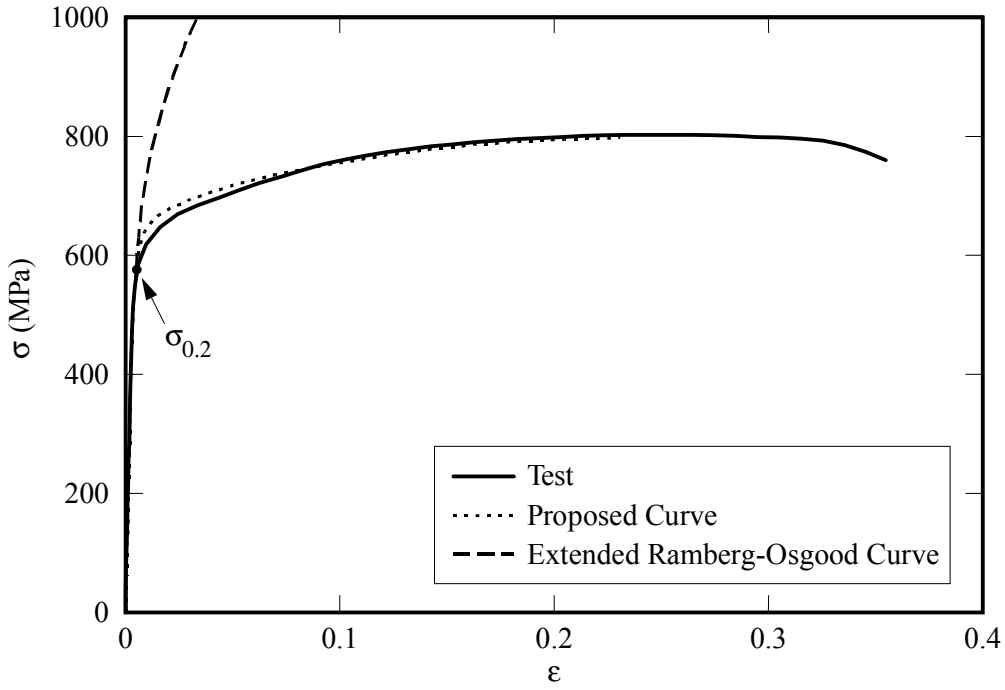

Figure 5. Stress-strain curves for UNS31803 alloy. Test #15, see Table 1 for source.

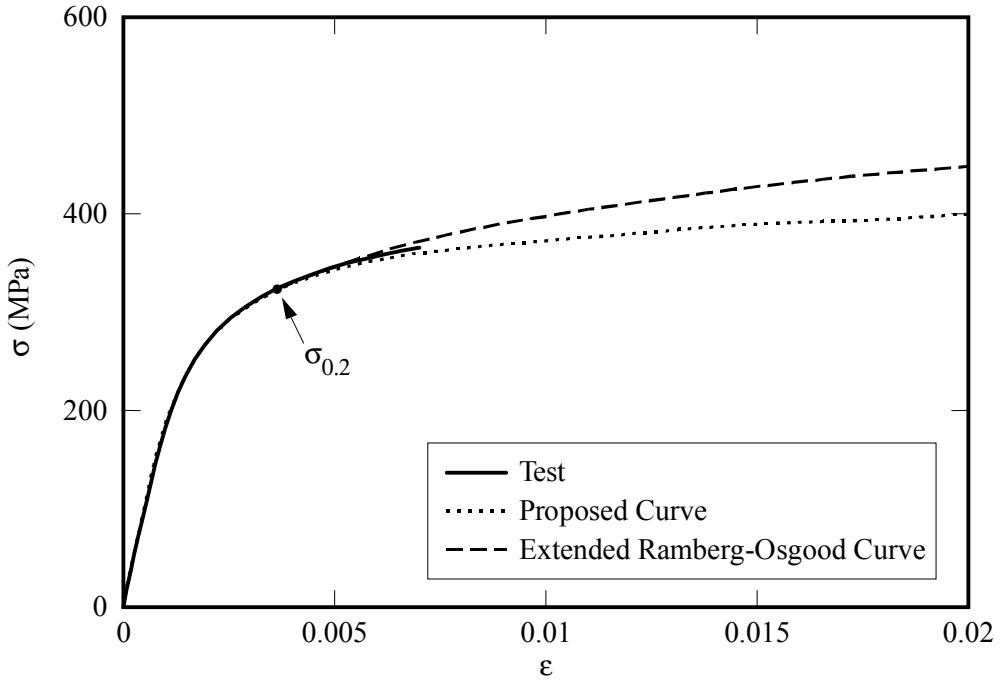

Figure 6. Stress-strain curves for UNS43000 alloy. Test #18, see Table 1 for source.

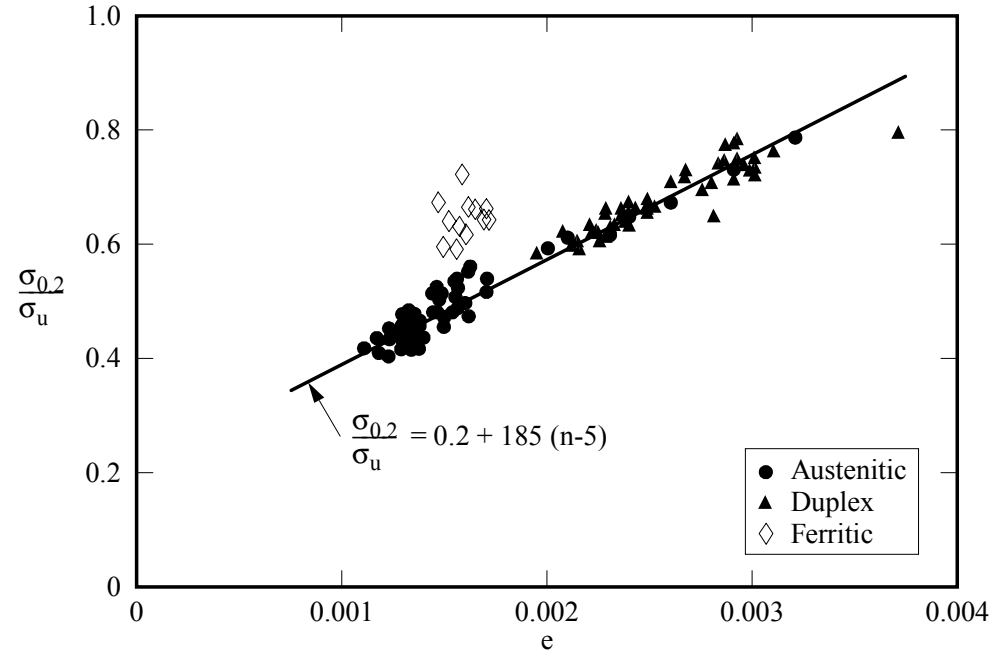

Figure 7. $\sigma_{0.2}/\sigma_u$ vs e. (The ferritic alloy test results are not included in the regression fit shown).

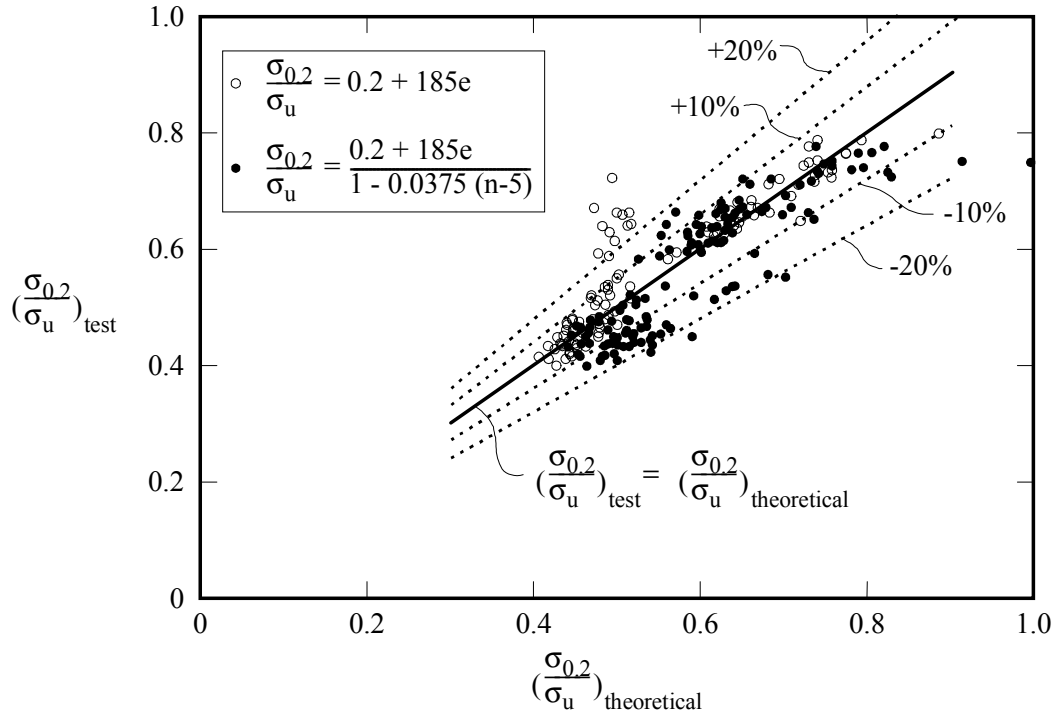

Figure 8. $(\sigma_{0.2}/\sigma_u)_{test}$ vs $(\sigma_{0.2}/\sigma_u)_{theoretical}$

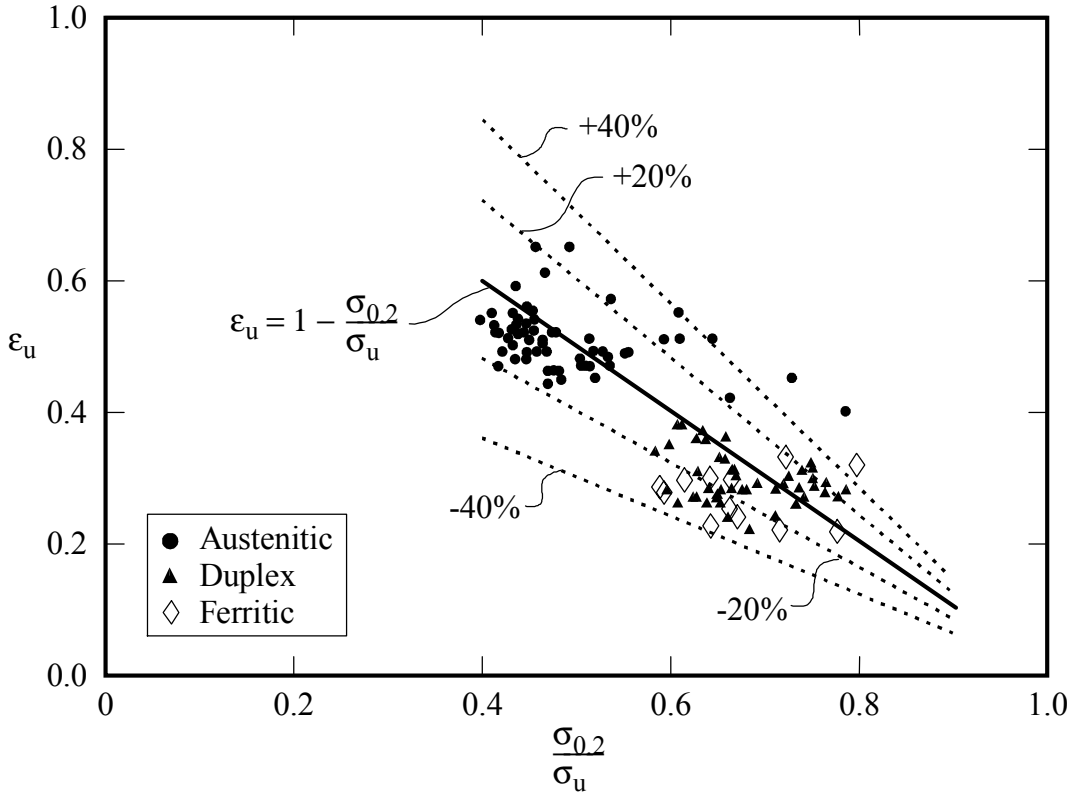

Figure 9: ε_u vs $(\sigma_{0.2}/\sigma_u)$

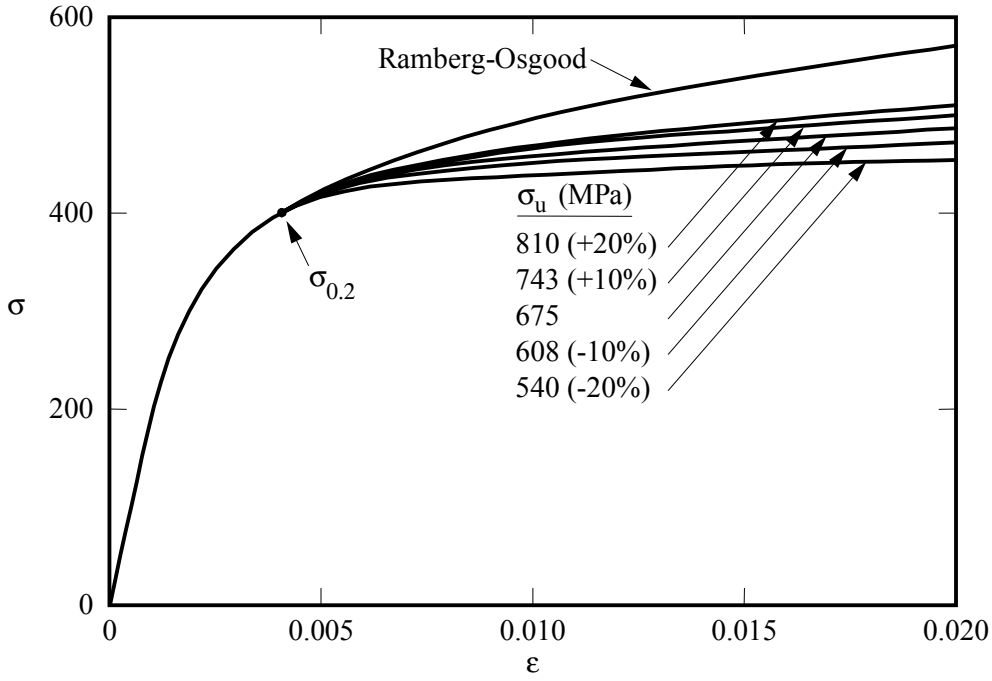

Figure 10: Effect of change in σ_u

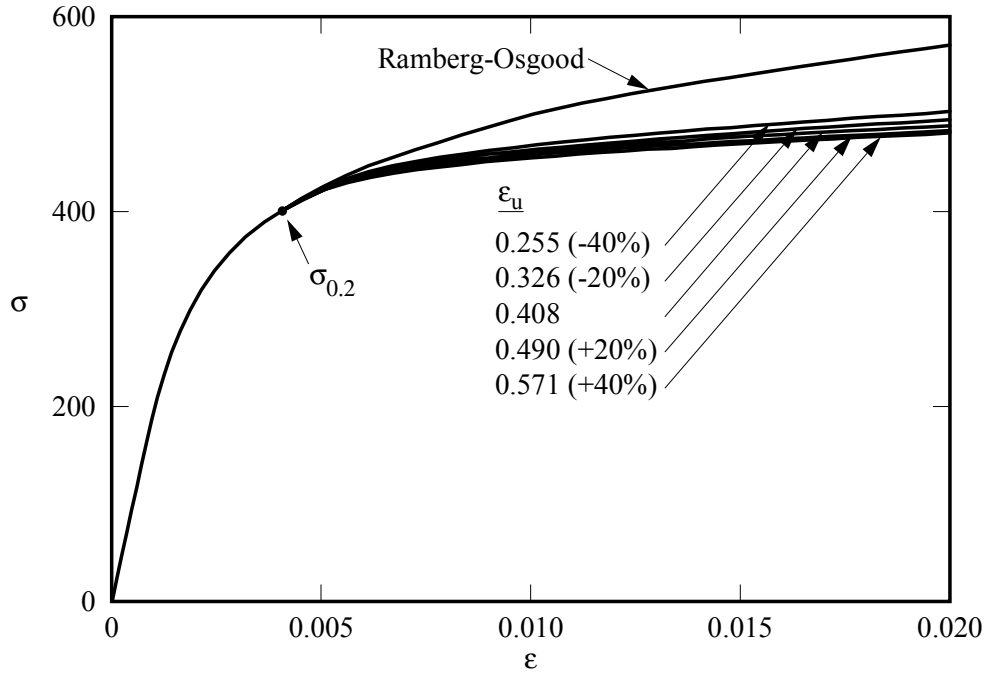

Figure 11: Effect of change in ε_u

Appendix A: Full-range Stress-strain Curves

This appendix contains comparisons of measured stress strain curves with stress-strain curves obtained using Eqn. 18. The test numbers given in the figure captions refer to Table 1. Where the full or large parts of the stress-strain curve was reported, comparisons are shown for the full and initial parts of the curve.

The first six measured stress-strain curves (Figs A.1-A.6) are obtained from Talja and Salmi (1995). The proposed curves in the same figures have been produced using the Ramberg-Osgood parameters (E_0, $\sigma_{0.2}$, n) also given in Talja and Salmi (1995). However, for Tests #3, 4 and 5, the Ramberg-Osgood parameters and stress-strain curves were not obtained from the same tests (although from nominally identical specimens) which probably explains the discrepancies seen in Figs A.3 and A.4. There is also some doubts about the Ramberg-Osgood parameters given in Talja and Salmi (1995) for Tests #1 and 2 in that the stress-strain curves do not intercept the 0.2% proof stress as required. However, despite these uncertainties, the *shape* of the proposed curves generally matches well the measured stress-strain curves, as shown in Figs A.1-A.6.

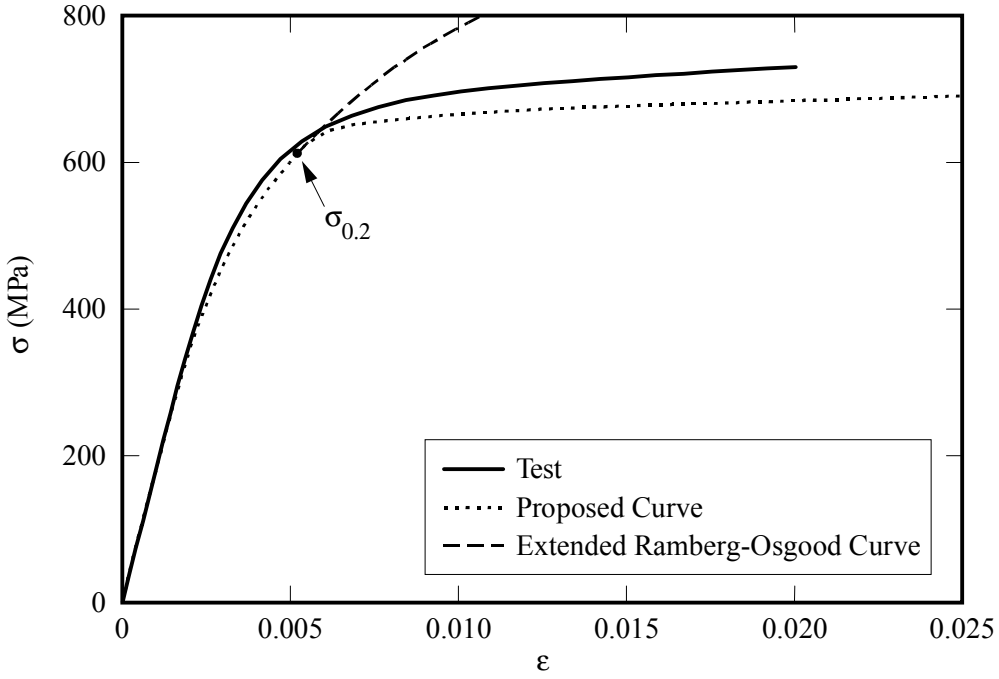

Figure A.1. Stress-strain curves for UNS30400 alloy. Test #1, (Talja & Salmi (1995), coupon RHS 1a-ST-1N).

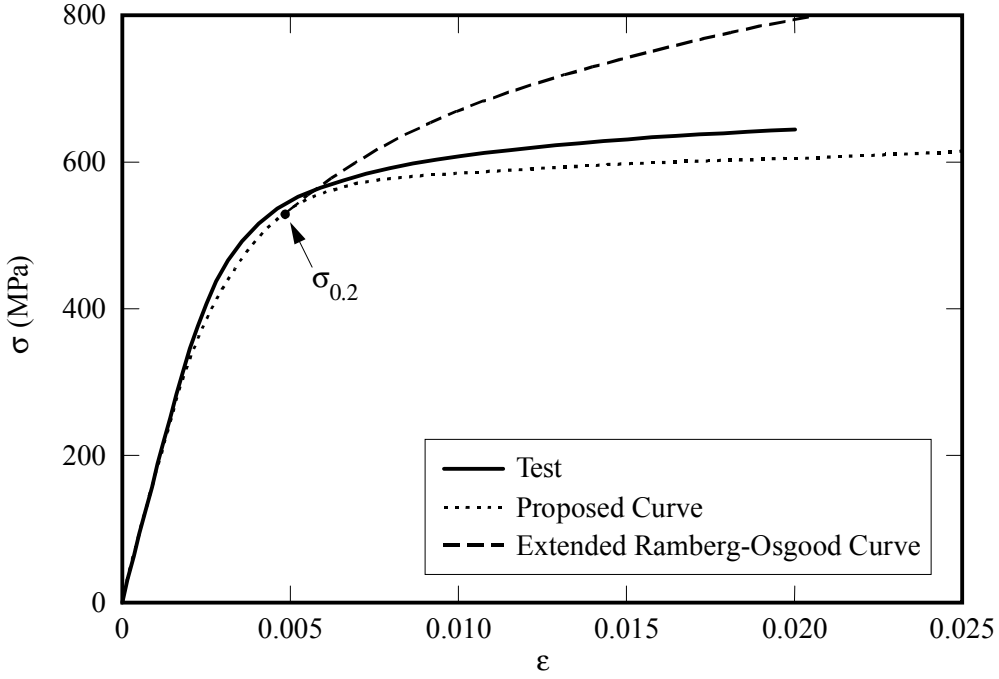

Figure A.2. Stress-strain curves for UNS30400 alloy. Test #2, (Talja & Salmi (1995), coupon RHS 1a-ST-1W).

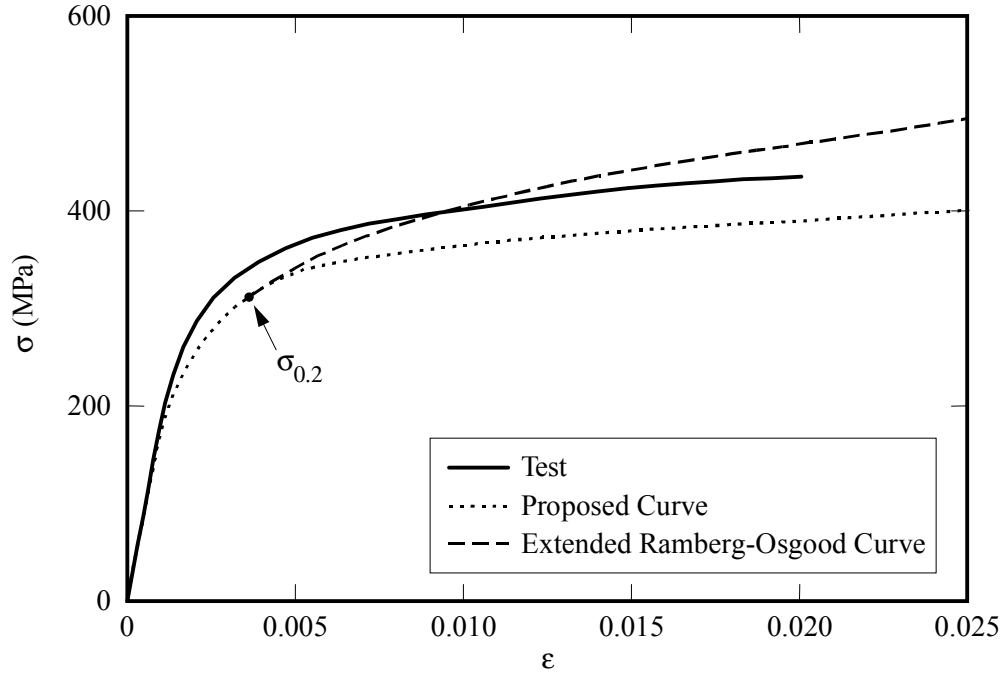

Figure A.3. Stress-strain curves for UNS30400 alloy. Test #3, (Talja & Salmi (1995), coupon RHS 2-ST-3N).

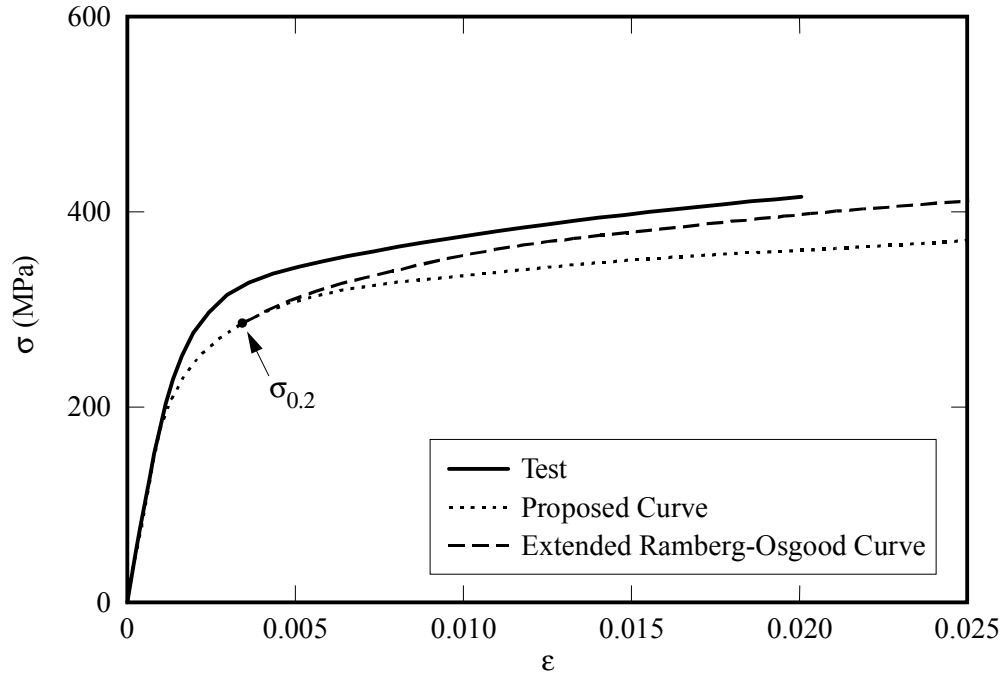

Figure A.4. Stress-strain curves for UNS30400 alloy. Test #4, (Talja & Salmi (1995), coupon RHS 2-ST-3W).

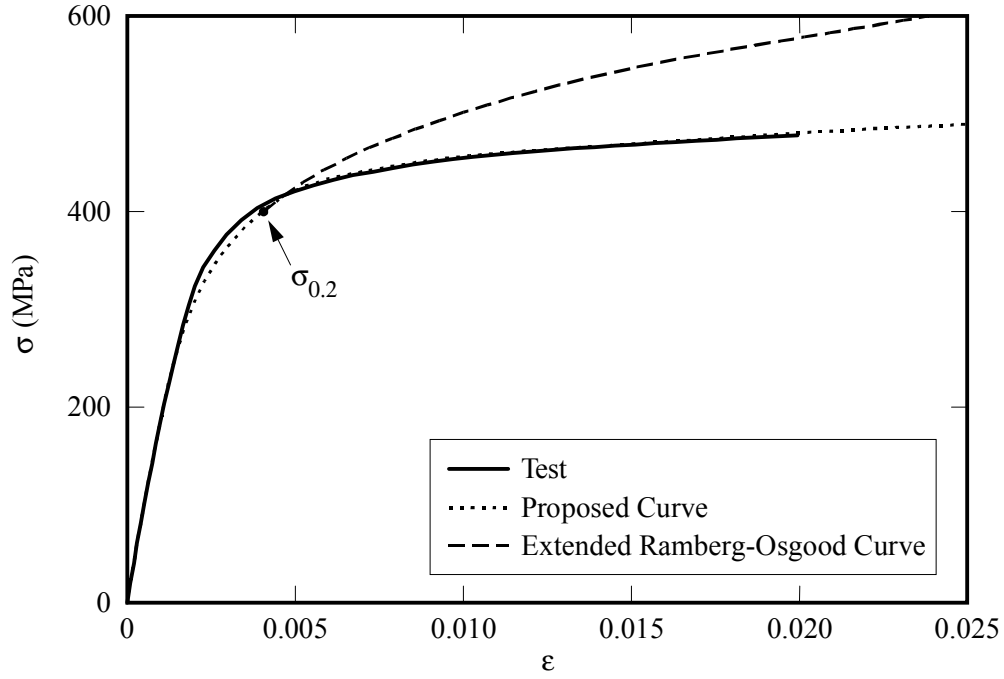

Figure A.5. Stress-strain curves for UNS30400 alloy. Test #5, (Talja & Salmi (1995), coupon RHS 3a-ST-2N).

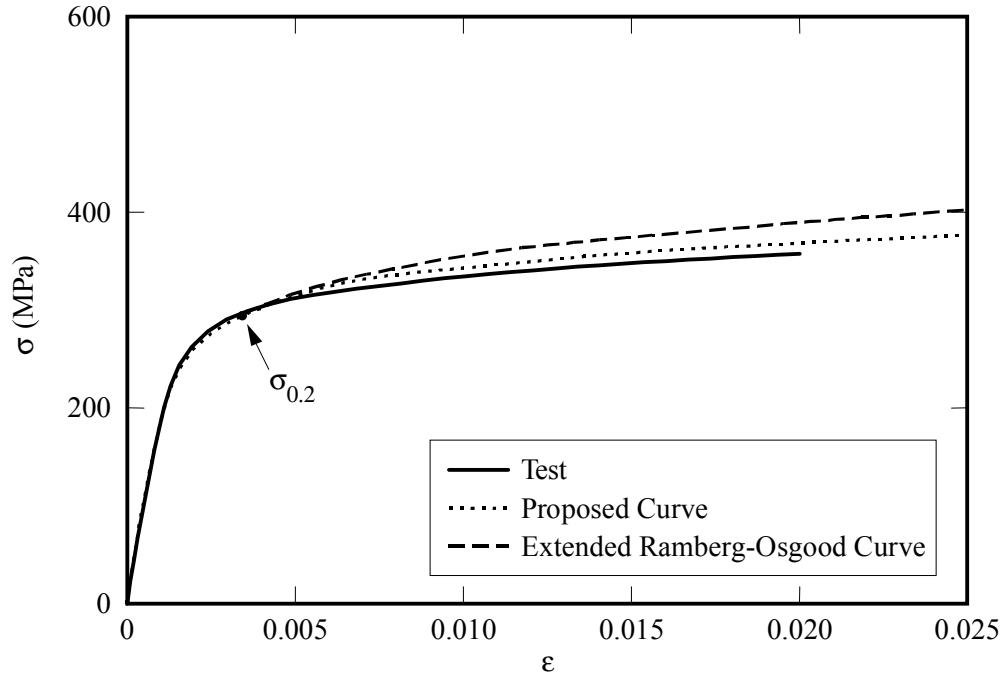

Figure A.6. Stress-strain curves for UNS30400 alloy. Test #6, (Talja & Salmi (1995), coupon RHS 3a-ST-2W).

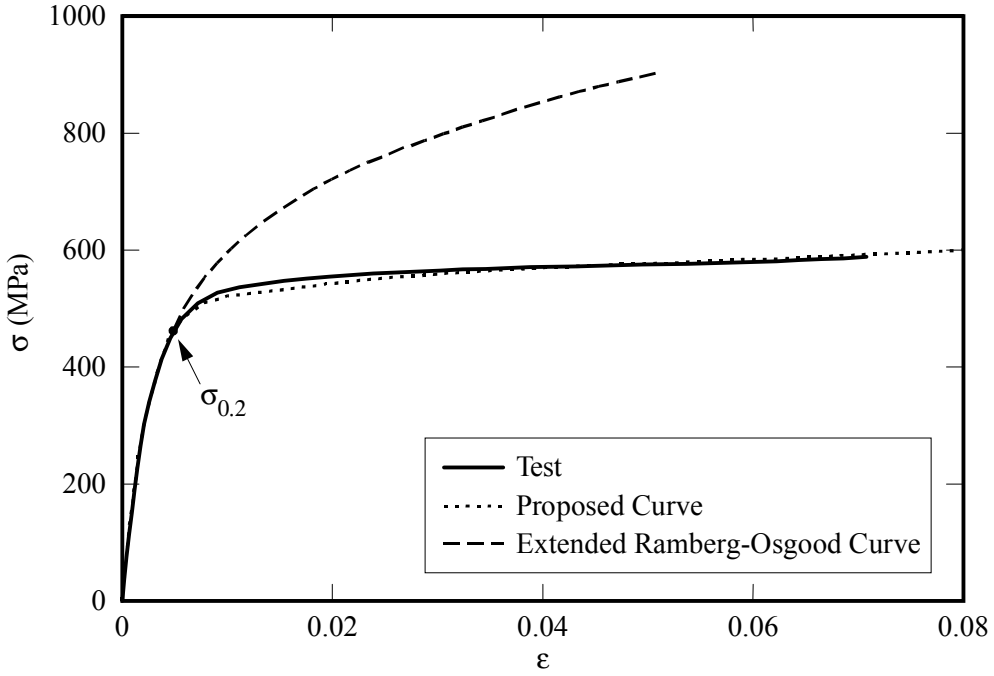

Figure A.7. Stress-strain curves for UNS30400 alloy. Test #7, (McDonald et al (2000), coupon W).

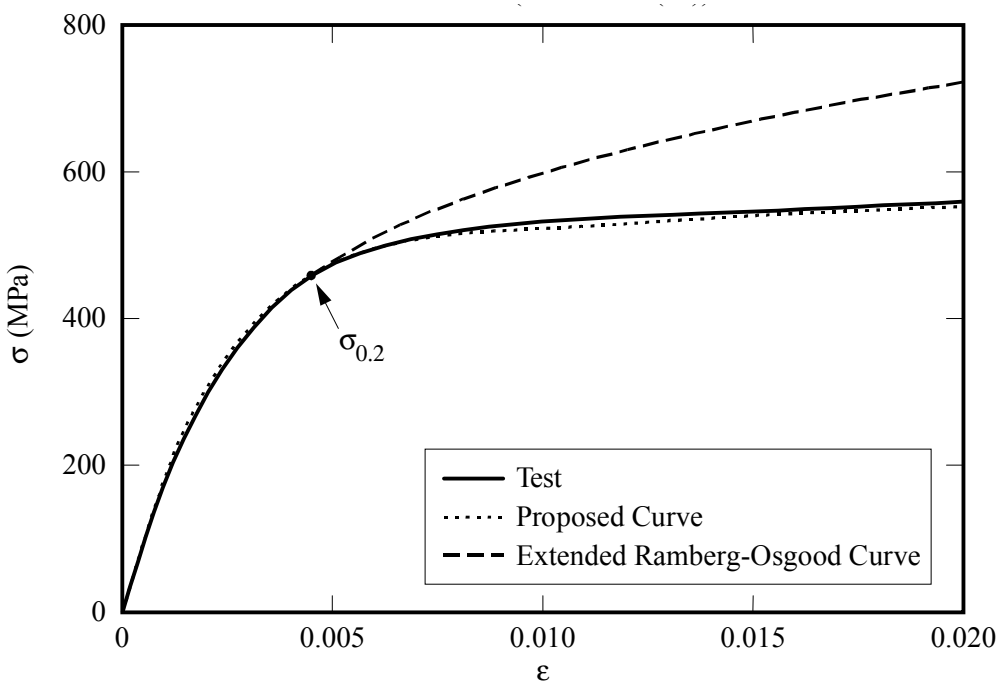

Figure A.8. Initial stress-strain curves for UNS30400 alloy. Test #7, (McDonald et al (2000), coupon W).

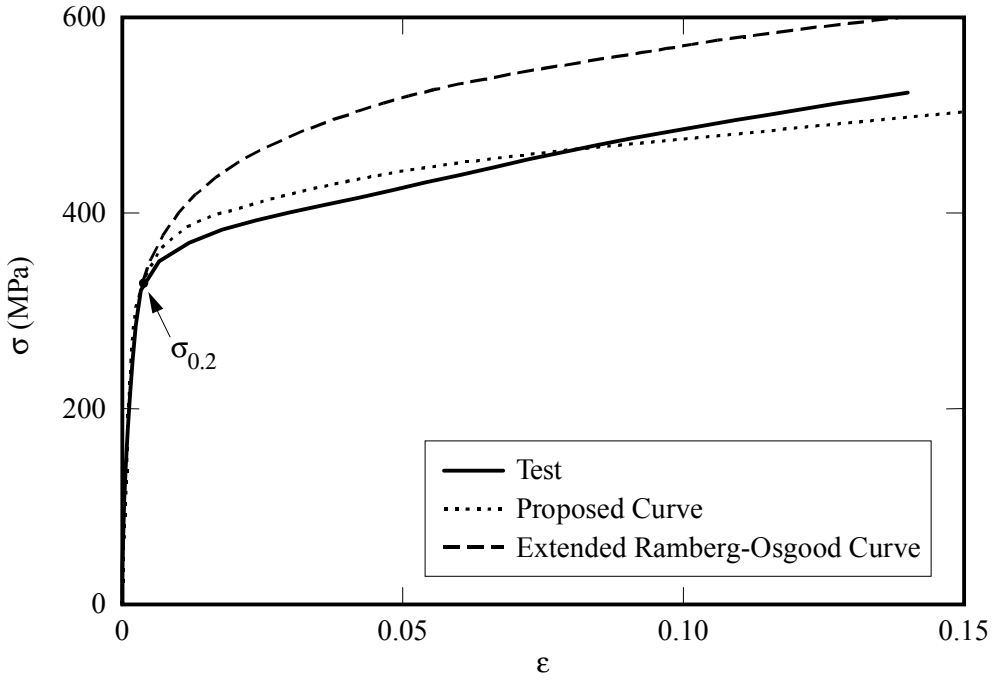

Figure A.9. Stress-strain curves for UNS30400 alloy. Test #8, (Olsson (2001), pp. 122 Fig. 5.6).

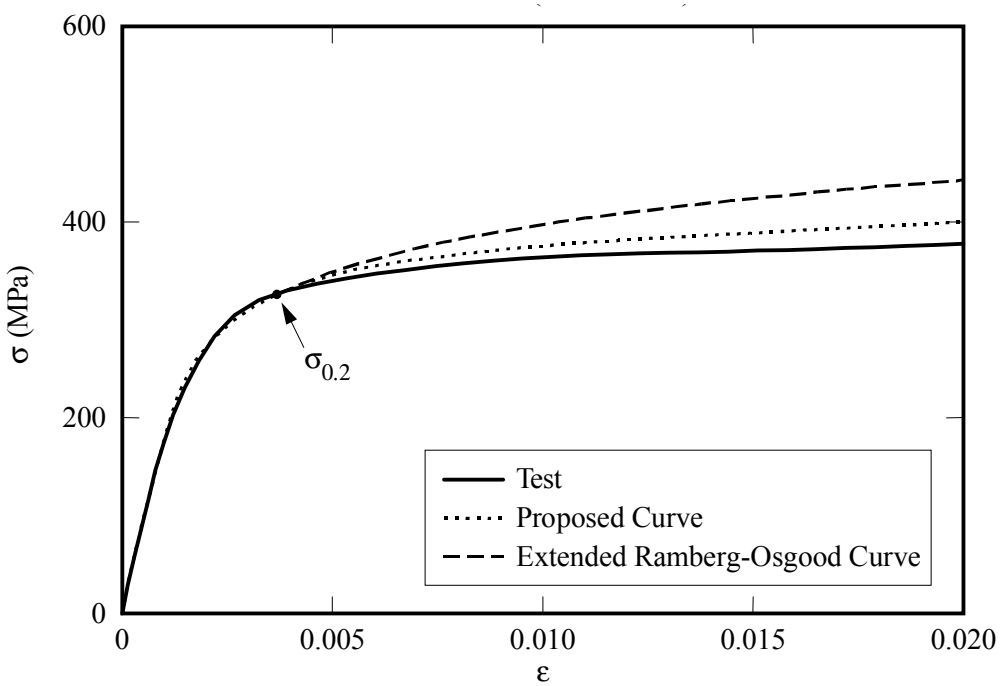

Figure A.10. Initial stress-strain curves for UNS30400 alloy. Test #8, (Olsson (2001), pp. 122 Fig. 5.6).

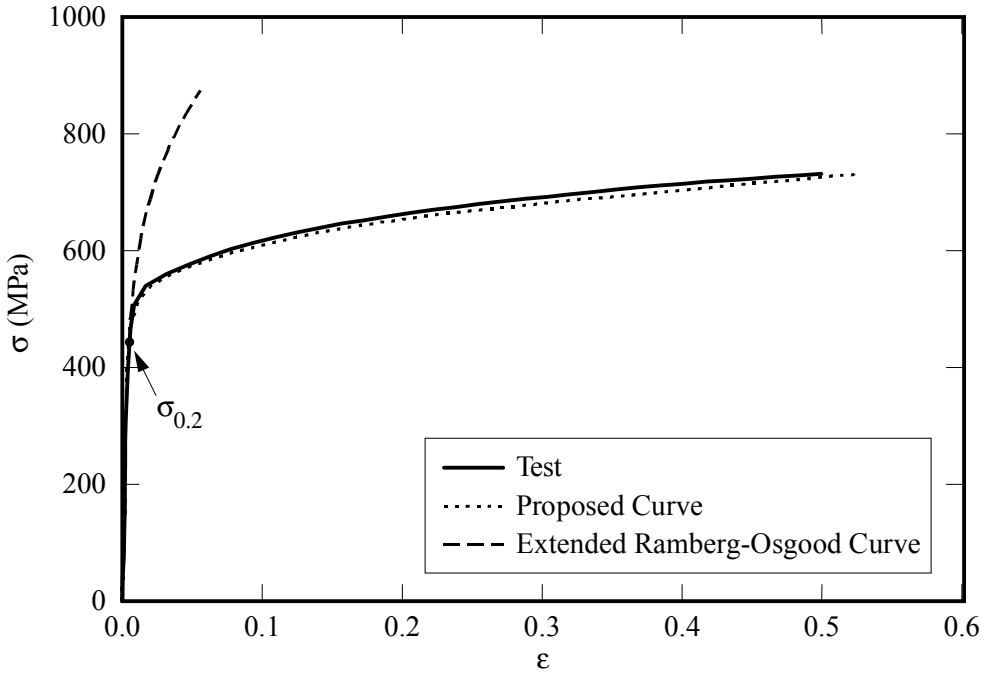

Figure A.11. Stress-strain curves for UNS30403 alloy. Test #9, (Rasmussen & Hancock (1993), Coupon T1-SHS).

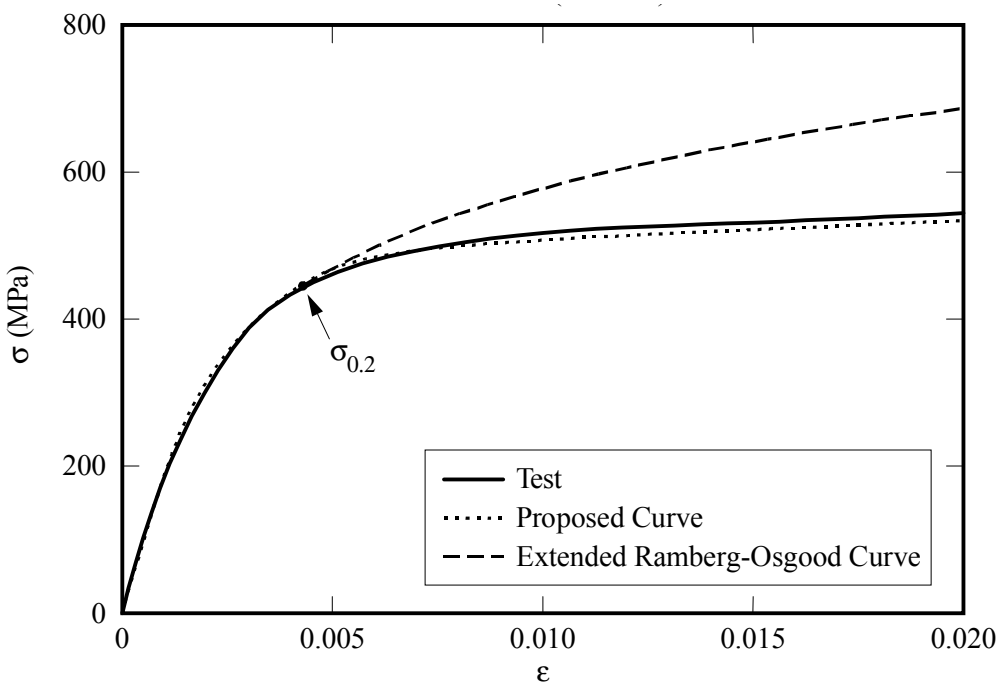

Figure A.12. Initial stress-strain curves for UNS30403 alloy. Test #9, (Rasmussen & Hancock (1993), Coupon T1-SHS).

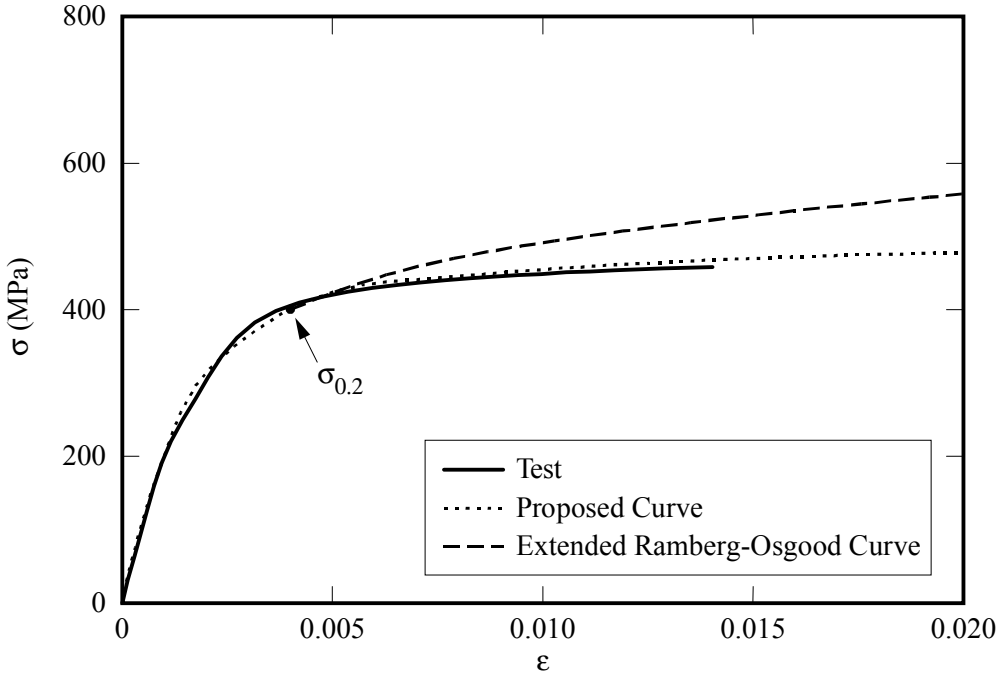

Figure A.13. Initial stress-strain curves for UNS30403 alloy. Test #10, (Rasmussen & Hancock (1993), Coupon C1-SHS).

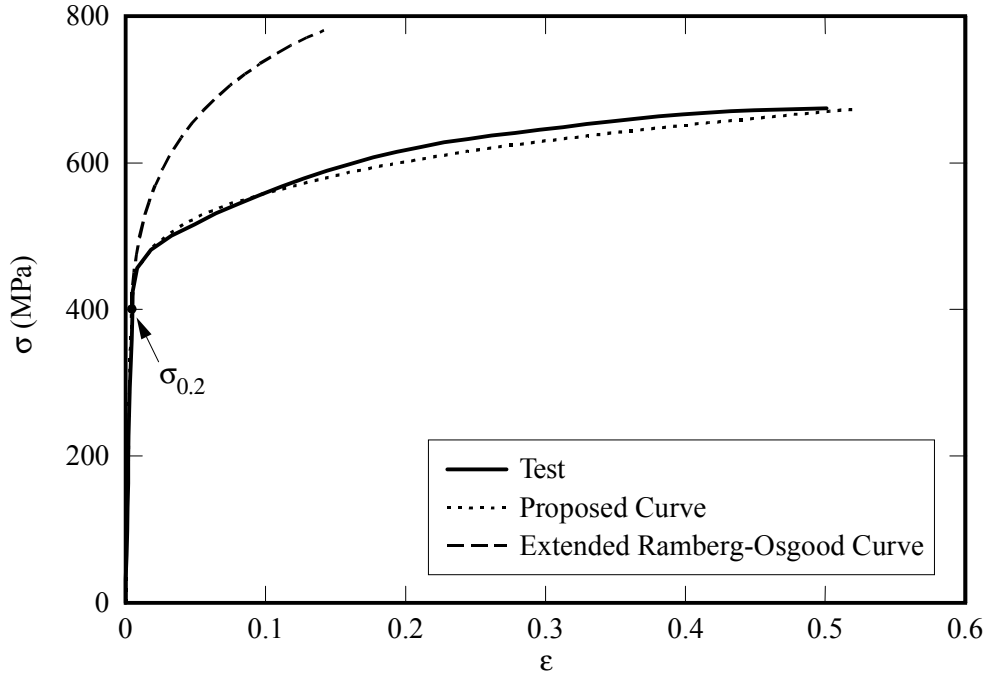

Figure A.14. Stress-strain curves for UNS30403 alloy. Test #11, (Rasmussen & Hancock (1993), Coupon T1-CHS).

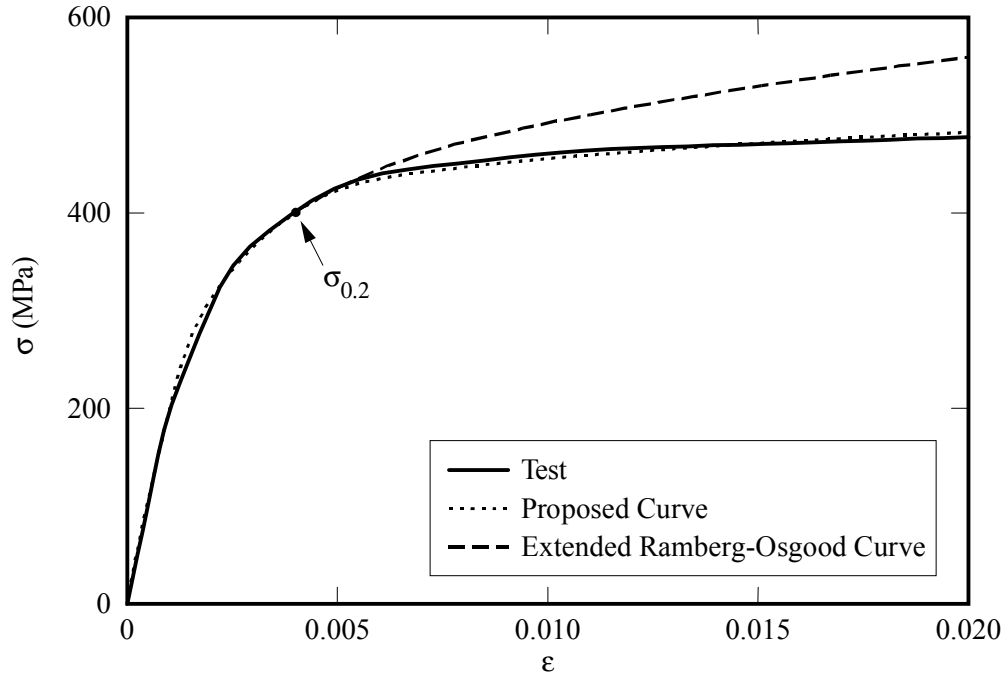

Figure A.15. Initial stress-strain curves for UNS30403 alloy. Test #11, (Rasmussen & Hancock (1993), Coupon T1-CHS).

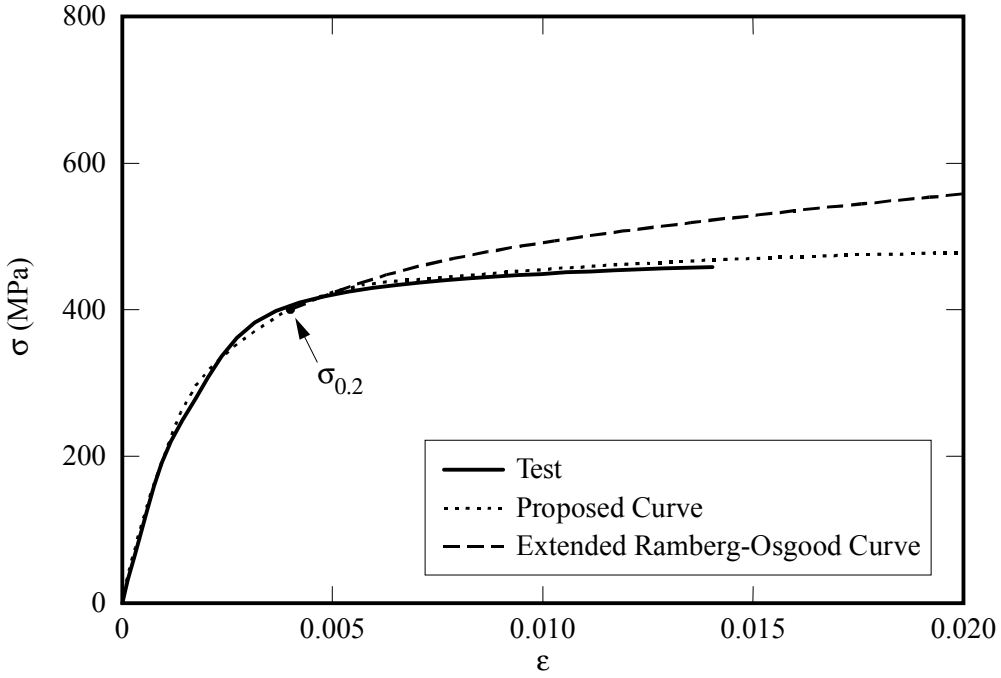

Figure A.16. Initial stress-strain curves for UNS30403 alloy. Test #12, (Rasmussen & Hancock (1993), Coupon C1-CHS).

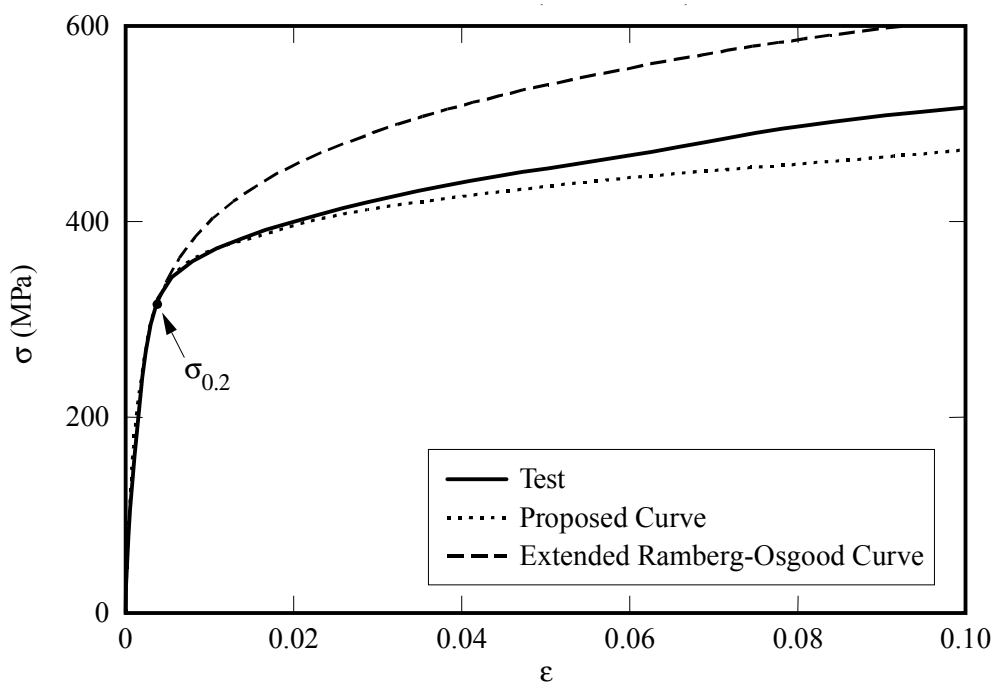

Figure A.17. Stress-strain curves for UNS31600 alloy. Test #13, (Olsson (2001), pp. 123, Fig. 5.7).

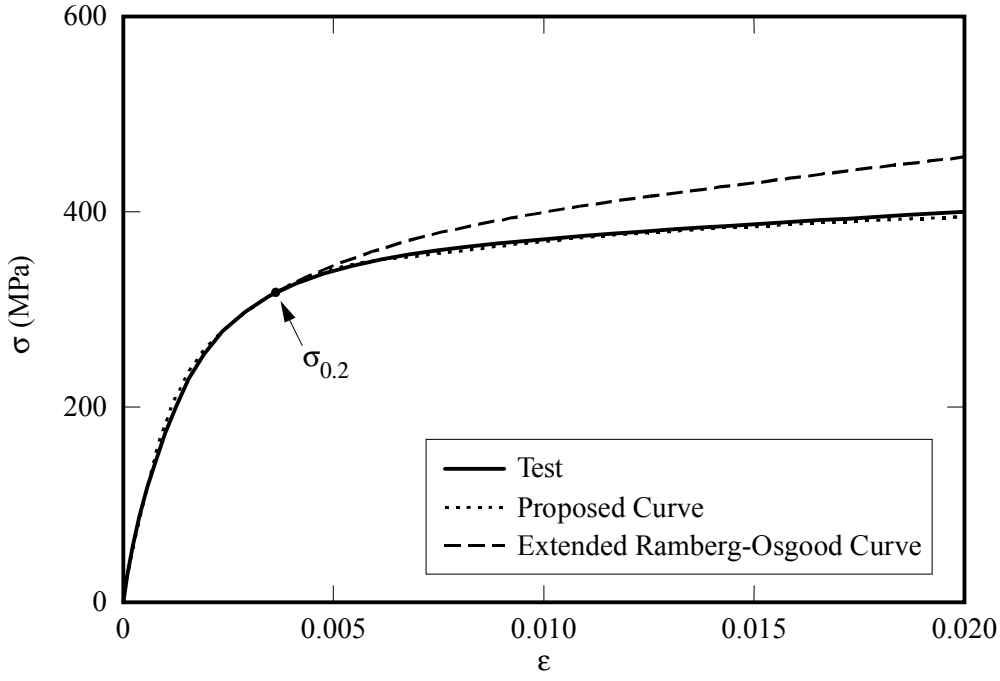

Figure A.18. Initial stress-strain curves for UNS31600 alloy. Test #13, (Olsson (2001), pp. 123, Fig. 5.7).

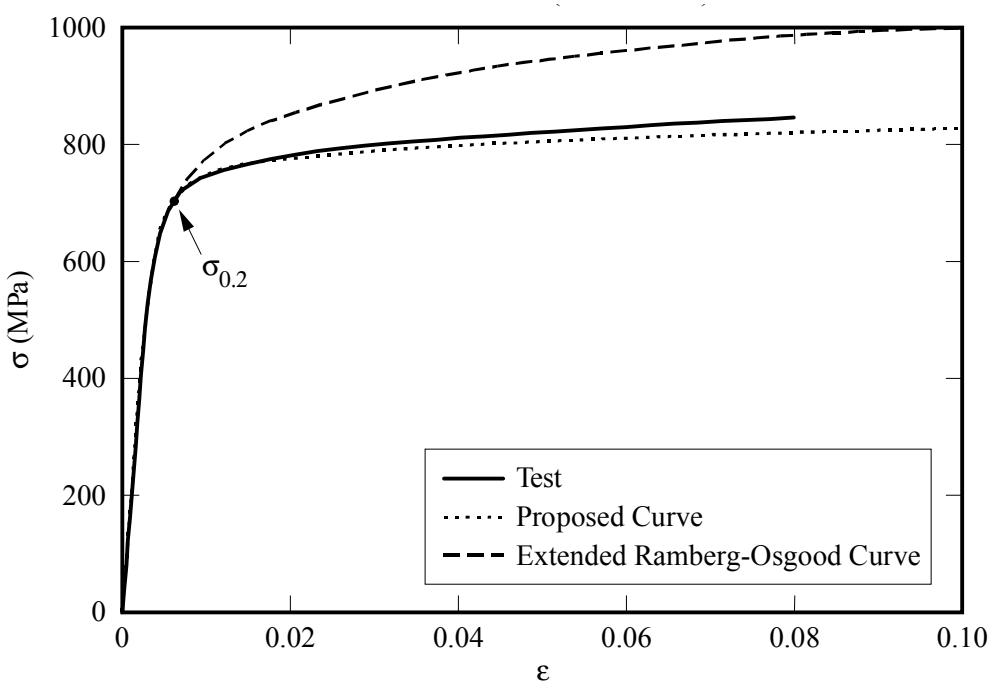

Figure A.19. Stress-strain curves for UNS31803 alloy. Test #14, (Olsson (2001), pp. 123, Fig. 5.8).

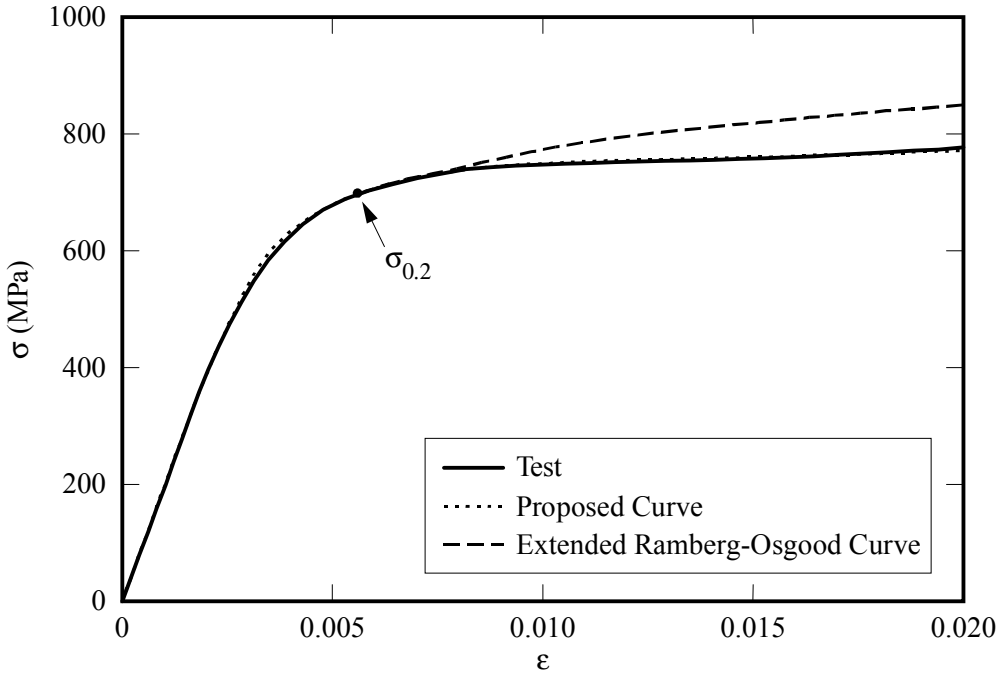

Figure A.20. Initial stress-strain curves for UNS31803 alloy. Test #14, (Olsson (2001), pp. 123, Fig. 5.8).

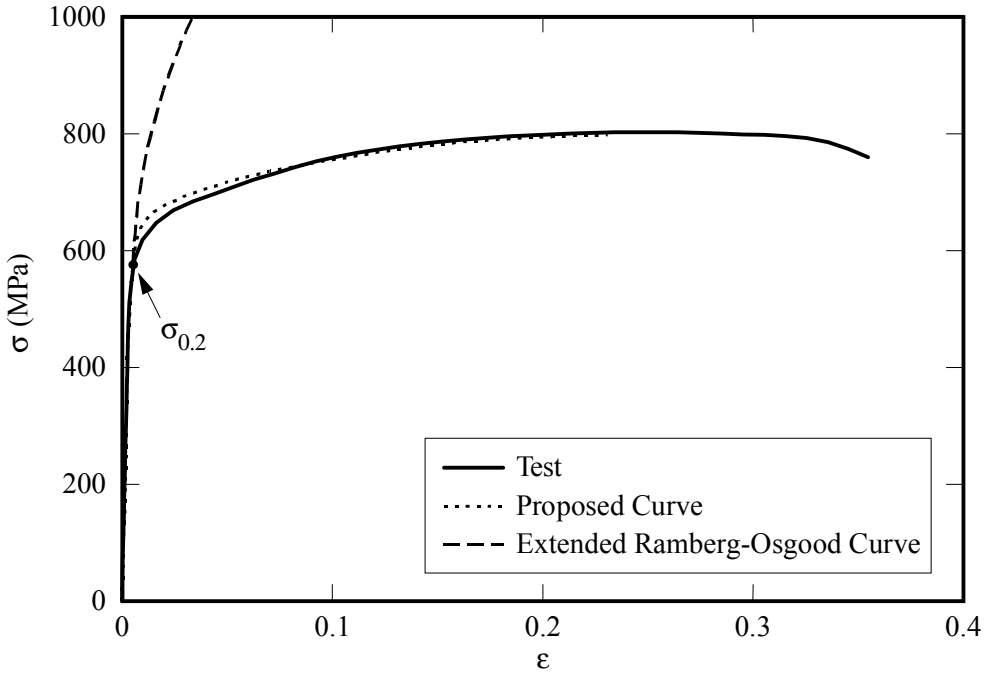

Figure A.21. Stress-strain curves for UNS31803 alloy. Test #15, (Burns & Bezkorovainy (2001), coupon LT2).

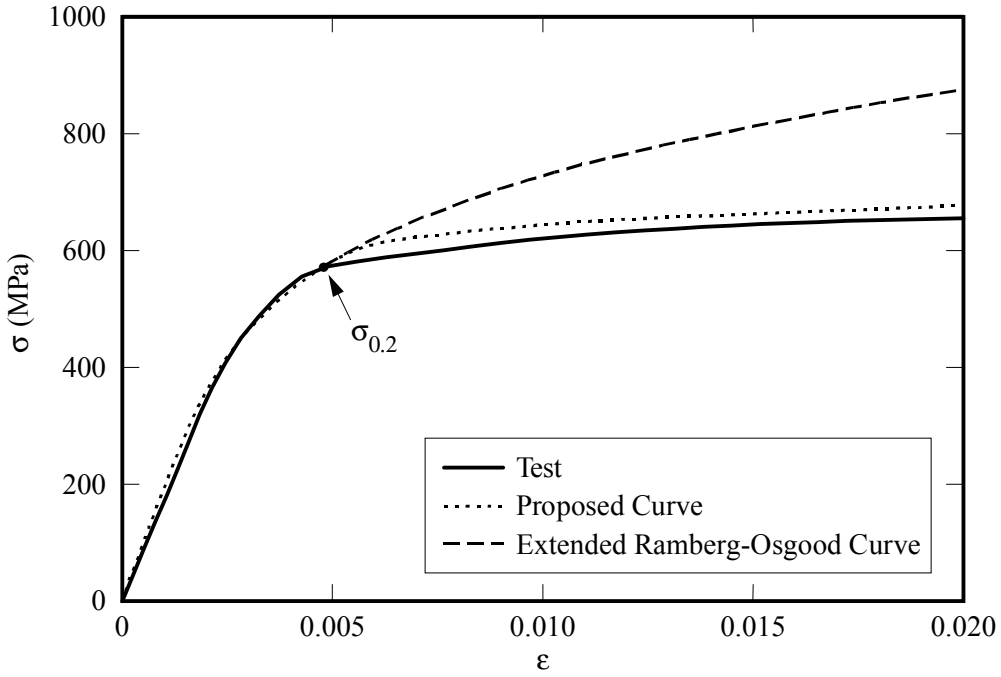

Figure A.22. Initial stress-strain curves for UNS31803 alloy. Test #15, (Burns & Bezkorovainy (2001), coupon LT2).

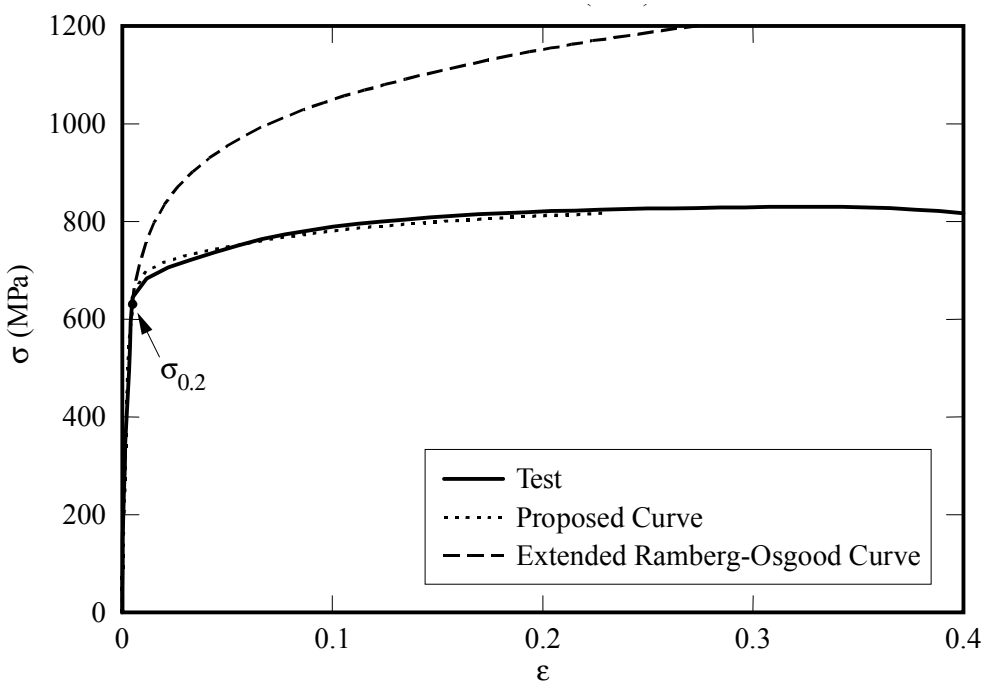

Figure A.23. Stress-strain curves for UNS31803 alloy. Test #16, (Burns & Bezkorovainy (2001), coupon TT1).

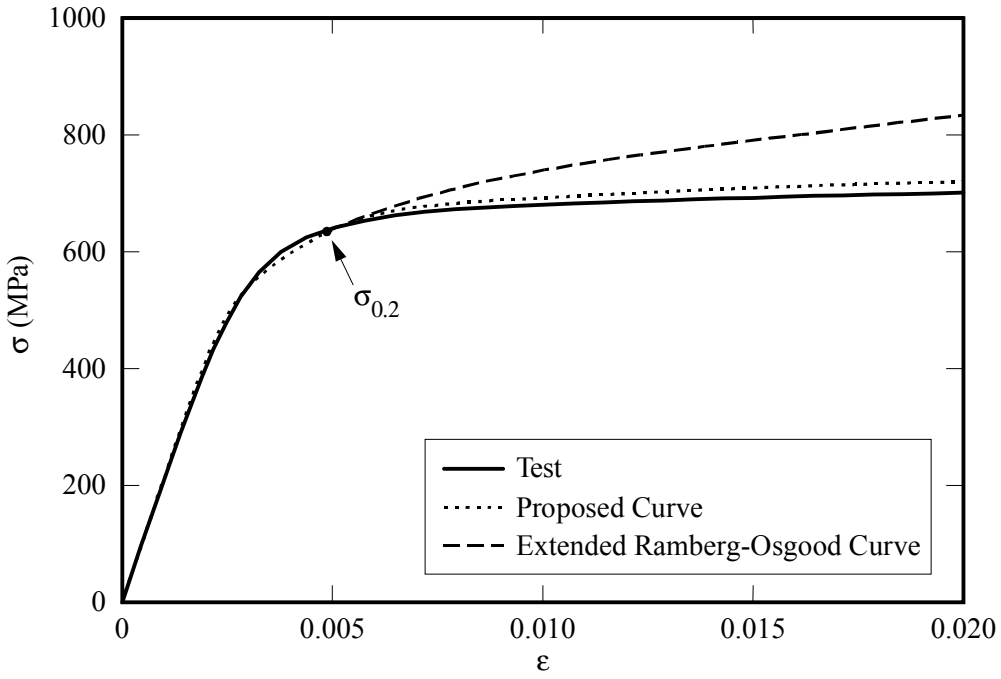

Figure A.24. Initial stress-strain curves for UNS31803 alloy. Test #16, (Burns & Bezkorovainy (2001), coupon TT1).

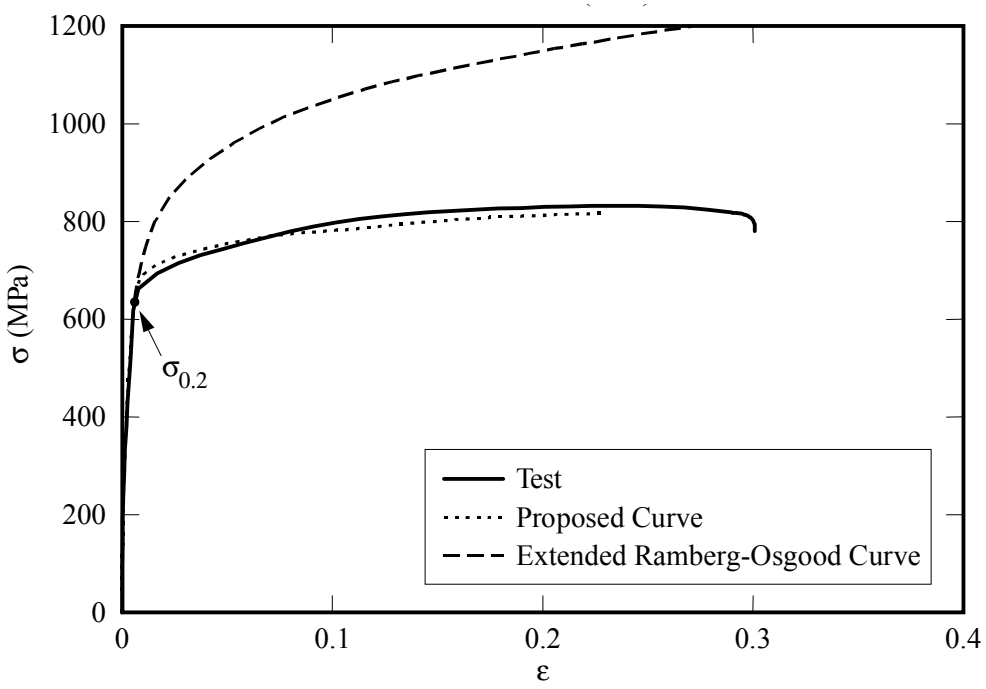

Figure A.25. Stress-strain curves for UNS31803 alloy. Test #17, (Burns & Bezkorovainy (2001), coupon TT2).

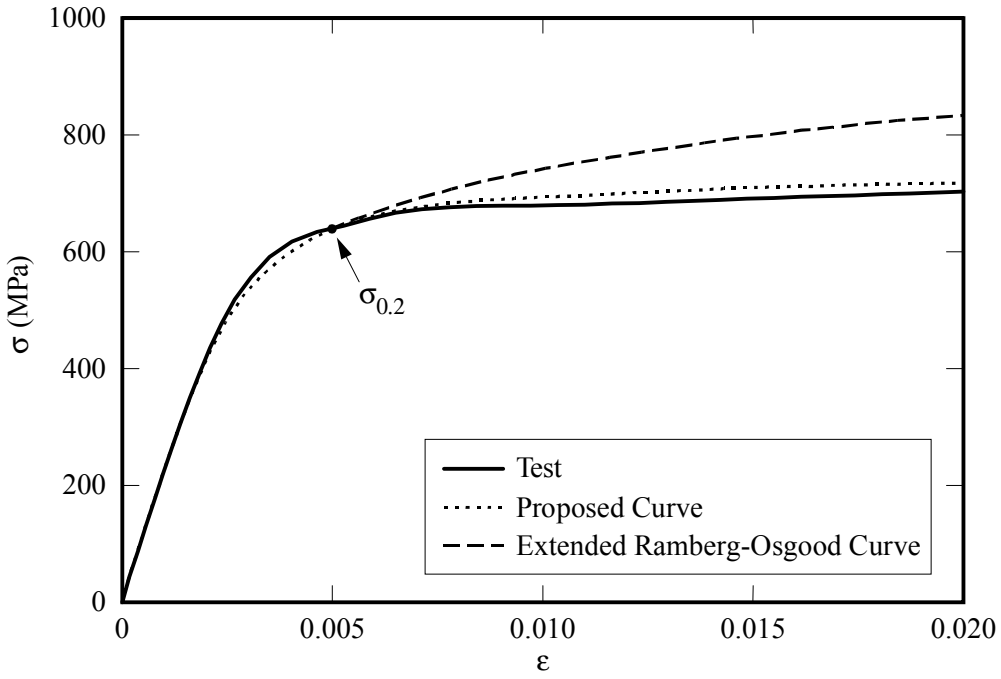

Figure A.26. Initial stress-strain curves for UNS31803 alloy. Test #17, (Burns & Bezkorovainy (2001), coupon TT2).

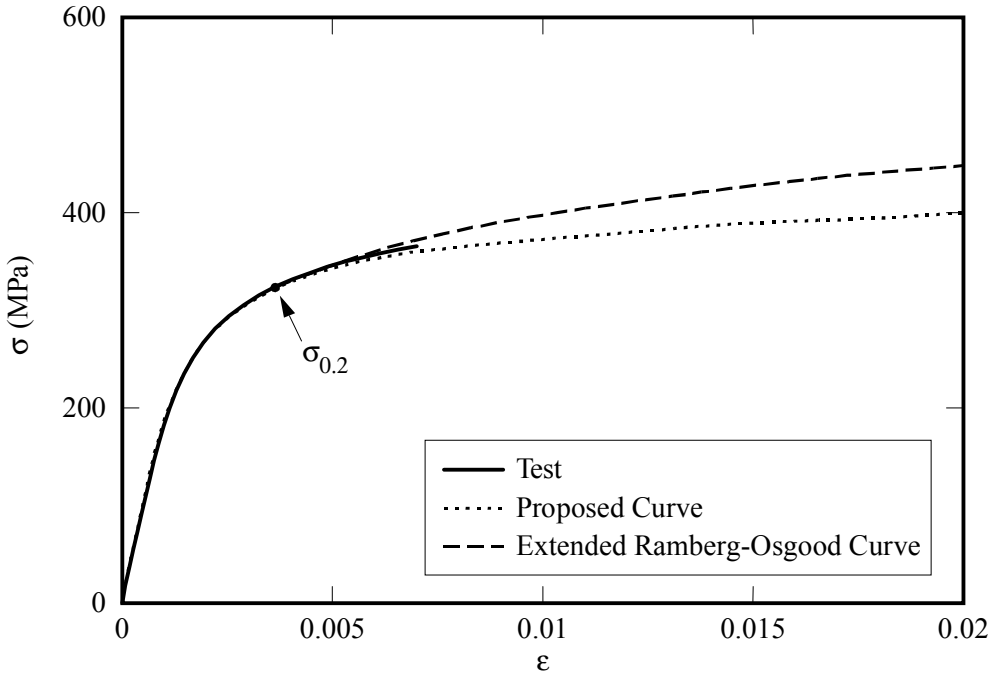

Figure A.27. Stress-strain curves for UNS43000 alloy. Test #18, (Korvink & van den Berg (1993), Coupon Type 430).

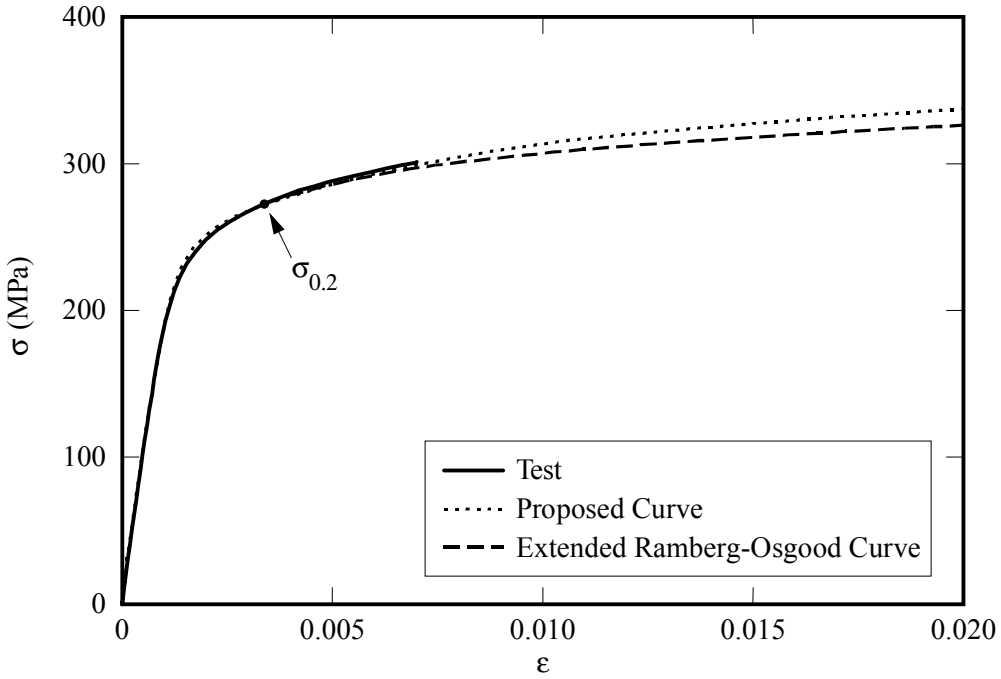

Figure A.28. Stress-strain curves for UNS43000 alloy. Test #19, (Korvink & van den Berg (1993), Coupon Type 3Cr12).

Appendix B: Coupon Test Data

Appendix B.1 summarises the test data contained in the report by the Steel Construction Institute (SCI, 1991).

Appendix B.2 summarises the test data contained in the reports by van der Merwe et al. (1986) and van der Merwe & van den Berg (1987) from Rand Afrikaans University. The data are the mean values given in the reports.

Appendix B.1: SCI Coupon Test Data

Alloy: 304L
Longitudinal Tension (LT)

Specimen	t (mm)	l. rate ($N/mm^2/s$)	$s_{0.2}$ MPa	$s_{1.0}$ MPa	s_u MPa	elong. %	E_0 GPa	n	$s_{0.01}/s_{0.2}$
LT1	1.9	3	269.1	309.3	619.0	48	200.9	5.5	0.58
LT2	1.9	3	267.1	307.0	618.6	51	189.3	6.4	0.63
LT3	1.9	3	266.1	307.8	639.8	52	194.2	6.7	0.64
LT1R	4	3	285.5	335.6	598.4	52	195.8	7.1	0.65
LT4R	4	3	255.7	303.1	588.4	59	199.4	6.7	0.64
LT1R	10	3	258.8	297.5	594.6	54	191.7	7.6	0.67
LT2R	10	0.3	247.8	287.4	606.2	55	193.1	7.3	0.66
LT3R	10	30	267.6	311.5	596.8	52	199.1	8.5	0.70
LT4R	10	3	247.4	293.4	598.7	52	186.1	5.5	0.58
LT5R	10	0.3	239.5	287.0	602.4	54	195.4	7.1	0.66
LT6R	10	30	272.1	315.0	300.6	55	195.9	8.2	0.70
LT1	9.53	3	258.8	293.0	568.5	54	188.5	7.9	0.69
LT2	9.53	0.3	242.9	278.1	563.2	55	208.5	8.7	0.71
LT3	9.53	30	253.6	289.0	567.5	56	190.5	7.8	0.68
Average			259.4	301.1	575.9	53.5	194.9	7.2	0.66
Standard deviation			12.72	14.79					
Coefficient of variation			0.049	0.049					

Transverse Tension (TT)

Specimen	t (mm)	l. rate (N/mm2/s)	$s_{0.2}$ MPa	$s_{1.0}$ MPa	s_u MPa	elong. %	E_0 GPa	n	$s_{0.01}/s_{0.2}$
TT1	1.9	3	264.9	305.2	605.2	54	201.8	9.3	0.72
TT2	1.9	0.03	260.3	296.8	594.3	52	203.2	9.2	0.72
TT3	1.9	30	279.7	308.6	603.9	51	201.2	10.0	0.74
TT4	1.9	3	270.0	311.4	601.4	51	180.8	10.1	0.74
TT5	1.9	0.03	261.1	321.6	601.4	52	194.9	9.6	0.73
TT6	1.9	30	279.9	320.2	604.1	50	210.6	9.1	0.72
TT7	1.9	3	265.7	304.8	601.5	53	201.5	9.7	0.73
TT1R	4	3	264.0	317.5	612.5	50	205.1	8.6	0.71
TT3R	4	30	278.0	335.1	608.4	49	208.9	7.3	0.66
TT4R	4	3	264.9	317.4	610	52	212.7	8.7	0.71
TT1	9.53	3	258.5	296.6	577.2	52	196.4	9.8	0.74
TT2	9.53	0.03	233.2	268.8	571.2	55	198.9	9.4	0.73
TT3	9.53	30	259.9	298.1	570.6	54	202.0	6.4	0.62
TT4	9.53	3	249.0	286.7	571	52	190.1	7.7	0.68
TT5	9.53	0.03	235.9	272	9.2	9	213.2	9.2	0.72
TT6	9.53	30	260.4	297.4	574.9	55	194.3	10.0	0.74
TT7	9.53	3	257.3	291.5	574.6	53	202.0	8.2	0.70
Average			261.3	302.9	558.3	49.7	201.0	9.0	0.71
Standard deviation			13.00	17.43					
Coefficient of variation			0.050	0.058					

Alloy: 304L
Longitudinal Compression (LC)

Specimen	t	l. rate	$s_{0.2}$	$s_{1.0}$	s_u	elong.	E_0	n	$s_{0.01}/s_{0.2}$
	(mm)	($N/mm^2/s$)	MPa	MPa	MPa	%	GPa		
LC1	4	3	252.3	307.0			216.5	5.9	0.60
LC2	4	0.3	247.4	308.4			181.8	5.3	0.57
LC3	4	30	270.4	322.3			176.0	7.0	0.65
LC4	4	3	254.6	309.4			207.0	5.6	0.58
LC5	4	0.3	249.4	308.8			164.3	6.9	0.65
LC6	4	30	269.0	323.8			159.9	6.8	0.64
LC7	4	3	255.2	309.8			189.9	6.0	0.60
LC1	10	3	245.3	289.3			198.2	6.3	0.62
LC2	10	0.3	240.0	285.1			178.0	6.2	0.62
LC3	10	30	260.1	308.0			195.3	5.4	0.57
LC4	10	3	247.3	295.2			182.5	6.1	0.61
LC5	10	0.3	236.4	279.1			184.5	6.7	0.64
LC6	10	30	257.9	303.8			170.9	7.6	0.67
LC7	10	3	245.9	288.3			201.9	6.6	0.63
LC1	9.53	3	247.7	285.5			185.8	7.7	0.68
LC2	9.53	3	244.8	285.5			192.3	7.5	0.67
LC3	9.53	3	237.9	275.7			190.7	6.6	0.63
Average			250.7	299.1			186.8	6.5	0.63
Standard deviation			9.70	14.69					
Coefficient of variation			0.039	0.049					

Transverse Compression (TC)

Specimen	t	l. rate	s0.2	s1.0	su	elong.	E0	n	s0.01/s0.2
	(mm)	(N/mm2/s)	MPa	MPa	MPa	%	GPa		
TC1	4	3	264.5	314.1			195.1	8.9	0.72
TC2	4	0.3	258.3	306.9			191.5	9.3	0.73
TC3	4	30	284.1	331.4			216.0	9.9	0.74
TC4	4	3	267.0	320.4			169.1	10.2	0.74
TC5	4	0.3	256.9	301.8			191.6	9.9	0.74
TC6	4	30	280.9	339.0			192.2	9.8	0.74
TC7	4	3	267.3	315.8			208.2	8.4	0.70
TC1	10	3	249.6	297.5			181.7	8.3	0.70
TC2	10	0.3	243.1	291.0			177.8	8.9	0.71
TC3	10	30	262.9	313.3			181.7	9.2	0.72
TC4	10	3	249.6	298.0			212.7	7.8	0.68
TC5	10	0.3	241.4	288.9			186.1	10.4	0.75
TC6	10	30	261.1	309.4			193.8	9.4	0.73
TC7	10	3	248.1	296.4			219.6	8.7	0.71
TC1	9.53	3	246.0	289.4			168.0	6.9	0.65
TC2	9.53	3	250.4	296.3			186.2	8.6	0.71
TC3	9.53	3	240.1	281.3			186.4	6.9	0.65
Average			257.1	305.3			191.6	8.9	0.71
Standard deviation			12.98	15.62					
Coefficient of variation			0.050	0.051					

Alloy: 316L
Longitudinal Tension (LT)

Specimen	t (mm)	l. rate ($N/mm^2/s$)	$s_{0.2}$ MPa	$s_{1.0}$ MPa	s_u MPa	elong. %	E_0 GPa	n	$s_{0.01}/s_{0.2}$
LT1	2	3	293.4	330.3	565.8	45	186.7	6.2	0.61
LT2	2	3	287.3	321.5	570.4	47	186.0	6.8	0.64
LT3	2	3	289.2	322.2	568.7	47	194.1	7.3	0.66
LT7	4	3	275.0	328.1	587.7	46	213.2	5.6	0.59
LT1R	4	3	268.5	311.7	574.3	49	199.7	5.4	0.57
LT4R	4	3	270.1	314.3	580.8	49	200.7	6.0	0.61
LT1	6	3	282.4	318.1	602.1	44	174.4	7.8	0.68
LT2	6	3	291.5	321.8	604.6	45	187.5	7.3	0.66
LT1R	10	3	252.8	296.3	585.7	50	185.5	7.9	0.68
LT2R	10	0.3	244.7	288.6	586.5	47	187.8	7.9	0.69
LT3R	10	30	265.1	307.4	584.8	52	195.4	5.8	0.59
LT4R	10	3	262.6	303.6	588.1	48	194.6	7.5	0.67
LT5R	10	0.3	248.1	291.1	590.3	49	189.4	9.8	0.74
LT6R	10	30	295.6	319.7	588.9	48	200.1	6.7	0.64
LT7R	10	3	260.6	295.3	579.5	52	196.9	8.8	0.71
Average			272.5	311.3	583.9	47.9	192.8	7.1	0.65
Standard deviation			16.92	13.58					
Coefficient of variation			0.062	0.044					

Transverse Tension (TT)

Specimen	t (mm)	l. rate (N/mm2/s)	s0.2 MPa	s1.0 MPa	su MPa	elong. %	E0 GPa	n	s0.01/s0.2
TT1	2	3	310.1	342.9	581.4	48	201.2	11.3	0.77
TT2	2	0.03	298.6	330.1	577.4	49	205.4	10.5	0.75
TT3	2	30	320.1	352.8	577.9	49	196.6	12.0	0.78
TT4	2	3	308.7	340.2	577.6	47	197.8	11.3	0.77
TT5	2	0.03	294.7	326.2	574.3	47	204.0	11.4	0.77
TT6	2	30	318.1	352.1	578.5	49	197.4	12.7	0.79
TT7	2	3	306.2	340.2	580.9	49	197.0	11.0	0.76
TT7	4	3	290.5	345.8	610.5	46	201.5	7.4	0.67
TT1R	4	3	289.1	345.8	612.5	46	211.7	6.4	0.63
TT4R	4	3	292.8	346.1	612.8	46	191.2	7.6	0.67
TT1	6	3	286.4	325.6	601.7	46	215.3	6.2	0.62
TT2	6	3	287.8	327.2	599.2	46	216.8	6.8	0.64
TT1R	10	3	257.7	303.1	576.3	49	210.6	7.1	0.66
TT2R	10	0.3	245.3	292.2	576.3	51	202.0	6.1	0.61
TT3R	10	30	274.0	319.7	579	52	213.0	7.9	0.69
TT5R	10	0.3	249.4	292.5	579.6	52	181.3	8.1	0.69
Average			289.3	330.2	587.2	48.3	202.7	9.0	0.70
Standard deviation			22.76	19.74					
Coefficient of variation			0.079	0.060					

Alloy: 316L
Longitudinal Compression (LC)

Specimen	t (mm)	l. rate ($N/mm^2/s$)	$s_{0.2}$ MPa	$s_{1.0}$ MPa	s_u MPa	elong. %	E_0 GPa	n	$s_{0.01}/s_{0.2}$
LC1	4	3	273.5	314.3			174.9	8.4	0.70
LC2	4	0.3	274.2	307.4			183.3	7.2	0.66
LC3	4	30	294.1	339.2			182.7	8.0	0.69
LC4	4	3	281.2	328.0			176.7	7.5	0.67
LC5	4	0.3	274.7	317.4			163.3	8.7	0.71
LC6	4	30	293.0	336.7			179.1	6.9	0.65
LC7	4	3	282.9	327.7			154.7	8.7	0.71
LC1	6	3	291.6	325.6			144.3	12.4	0.78
LC2	6	3	297.3	334.8			150.6	10.5	0.75
LC1R	6	3	296.0	335.7			177.8	11.2	0.77
LC2R	6	3	305.6	349.3			187.1	10.1	0.74
LC1	10	3	243.2	321.4			183.9	3.2	0.40
LC2	10	3	245.2	320.0			168.1	3.3	0.41
LC3	10	3	250.1	319.5			162.8	3.5	0.42
LC1	10	3	260.6	307.0			115.9	9.1	0.72
LC2	10	0.3	247.7	291.7			173.8	5.7	0.59
LC3	10	30	275.5	318.8			186.0	8.7	0.71
LC4	10	3	253.4	291.7			178.0	8.3	0.70
LC5	10	0.3	243.8	287.5			180.5	10.3	0.75
LC6	10	30	264.9	298.6			216.0	11.0	0.76
LC7	10	3	251.2	286.0			218.6	6.6	0.63
Average			271.4	317.1			174.2	8.1	0.66
Standard deviation			20.31	18.15					
Coefficient of variation			0.075	0.057					

Alloy: 316L

Transverse Compression (TC)

Specimen	t (mm)	l. rate ($N/mm^2/s$)	$s_{0.2}$ MPa	$s_{1.0}$ MPa	s_u MPa	elong. %	E_0 GPa	n	$s_{0.01}/s_{0.2}$
TC1	4	3	301.6	339.3			178.9	11.2	0.76
TC2	4	0.3	295.2	336.6			187.5	12.1	0.78
TC3	4	30	314.3	356.8			194.8	12.6	0.79
TC4	4	3	301.7	339.5			188.4	12.3	0.78
TC5	4	0.3	294.2	339.1			184.8	11.1	0.76
TC6	4	30	312.5	351.4			194.6	12.9	0.79
TC7	4	3	302.4	342.6			185.3	13.7	0.80
TC1	6	3	301.1	340.9			198.7	8.6	0.71
TC2	6	3	297.1	333.7			175.9	11.4	0.77
TC1	10	3	287.2	341.0			199.4	9.5	0.73
TC2	10	3	285.9	342.2			194.9	7.3	0.66
TC3	10	3	293.4	355.0			191.9	7.0	0.65
TC1	10	3	269.9	307.0			181.2	10.8	0.76
TC2	10	0.3	254.9	295.5			180.6	11.2	0.77
TC3	10	30	276.1	314.7			193.1	9.4	0.73
TC4	10	3	262.4	303.6			179.7	9.3	0.73
TC5	10	0.3	259.7	292.8			191.0	9.1	0.72
TC6	10	30	283.5	317.3			201.8	9.3	0.73
TC7	10	3	263.9	304.4			193.6	10.5	0.75
TC1	9.53	3	303.8	352.8			202.2	9.2	0.72
TC2	9.53	3	256.0	296.0			199.5	9.3	0.72
TC3	9.53	3	273.2	317.1			202.4	10.5	0.75
Average			285.9	328.2			190.9	10.4	0.74
Standard deviation			18.61	21.03					
Coefficient of variation			0.065	0.064					

Alloy: 2205
Longitudinal Tension (LT)

Specimen	t	l. rate	$s_{0.2}$	$s_{1.0}$	s_u	elong.	E_0	n	$s_{0.01}/s_{0.2}$
	(mm)	($N/mm^2/s$)	MPa	MPa	MPa	%	GPa		
LT1	2	3	594.4	663.3	823.6	30	197.7	7.3	0.67
LT2	2	3	595.3	662.0	815.9	30	199.7	7.3	0.66
LT3	2	3	604.4	674.7	820.0	31	204.6	6.6	0.63
LT1	5	3	572.8	624.6	770.3	31	202.7	5.8	0.59
LT2	5	0.3	580.4	627.4	776.5	32	203.3	12.2	0.78
LT3	5	30	581.7	629.5	776.9	31	193.4	9.5	0.73
LT1	4.75	3	465.7	585.6	745.6	27	208.6	4.3	0.50
LT2	4.75	0.03	448.6	566.0	755.0	28	207.8	4.2	0.49
LT3	4.75	30	490.9	607.4	752.6	28	206.1	4.9	0.54
LT4	4.75	3	472.3	596.4	743.3	26	197.5	4.5	0.52
LT5	4.75	0.03	450.7	563.1	744.1	26	210.3	4.6	0.52
LT6	4.75	30	491.9	604.4	754.1	26	208.8	4.8	0.53
LT7	4.75	3	476.5	594.6	747.3	28	216.6	4.7	0.53
LT1	12	3	467.6	569.1	747.0	36	202.2	5.4	0.57
LT2	12	0.03	458.4	564.4	751.0	38	201.8	4.7	0.53
LT3	12	30	452.5	562.0	747.2	38	201.3	4.1	0.48
LT1R	10	3	485.9	572.2	747.6	33	207.1	4.7	0.53
LT4R	10	3	481.1	562.0	732.9	33	194.4	4.9	0.50
LT7R	10	3	486.3	564.4	732.1	31	206.5	5.4	0.57
Average			508.3	599.6	762.3	30.7	203.7	5.8	0.6
Standard deviation			57.51	37.75	28.32	3.73	5.77	2.07	0.08
Coefficient of variation			0.113	0.063	0.037	0.121	0.028	0.358	0.148

Alloy: 2205
Transverse Tension (TT)

Specimen	t (mm)	l. rate ($N/mm^2/s$)	$s_{0.2}$ MPa	$s_{1.0}$ MPa	s_u MPa	elong. %	E_0 GPa	n	$s_{0.01}/s_{0.2}$
TT1	2	3	620.8	697.1	844.9	28	206.3	5.8	0.60
TT2	2	0.03	596.1	673.3	919.5	27	212.5	5.6	0.59
TT3	2	30	644.0	722.7	842.5	29	207.8	6.0	0.60
TT4	2	3	618.1	689.3	835.4	27	209.8	5.4	0.58
TT5	2	0.03	592.5	669.5	859.2	29	215.6	4.7	0.53
TT6	2	30	641.7	723.0	842.3	28	207.1	5.5	0.58
TT7	2	3	613.5	699.5	838.6	26	211.4	5.0	0.55
TT1	5	3	629.9	670.9	812.5	27	220.3	5.3	0.57
TT2	5	0.03	576.0	655.0	812.9	24	206.1	5.1	0.56
TT3	5	30	614.0	695.9	818.7	29	210.5	5.6	0.59
TT4	5	3	583.3	670.8	812.8	29	218.7	4.6	0.52
TT5	5	0.03	568.8	613.7	777.6	30	212.7		
TT6	5	30	612.8	667.3	781.1	28	210.1	12.1	0.78
TT7	5	3	578.5	667.3	814.6	28	222.6	4.1	0.48
TT1	4.75	3	492.4	619.4	771.5	26	207.3	4.1	0.48
TT2	4.75	0.03	481.0	607.4	772.4	27	232.0	3.5	0.43
TT3	4.75	30	526.8	641.1	772.6	22	211.9	4.4	0.51
TT4	4.75	3	512.6	627.8	778.5	24	214.5	3.9	0.47
TT5	4.75	0.03	485.2	602.1	780.4	27	216.3	3.6	0.44
TT6	4.75	30	533.2	645.0	785.8	28	223.1	4.2	0.49
TT7	4.75	3	513.0	626.5	779.7	28	204.9	4.0	0.48
TT1	12	3	487.2	594.1	777.2	31	221.1	3.9	0.46
TT2	12	0.03	451.5	570.5	775.5	34	232.2	3.2	0.39
TT3	12	30	511.9	618.1	779.1	36	225.4	4.0	0.47
TT4	12	3	494.8	596.0	777.5	36	215.3	4.4	0.51
TT5	12	0.03	462.6	567.6	774.7	35	218.5	3.6	0.43
TT6	12	30	520.9	628.7	780.6	31	214.5	4.1	0.48
TT7	12	3	491.2	594.9	776.9	37	211.9	4.4	0.50
TT1R	10	3	510.0	595.6	760.3	28	205.5	4.6	0.52
TT4R	10	3	508.9	596.4	761.1	30	201.3	5.4	0.57
TT7R	10	3	512.6	590.7	770.2	28	224.9	5.1	0.56
Average			547.9	639.9	799.6	28.9	214.6	4.8	0.5
Standard deviation			58.52	44.24	36.25	3.55	7.80	1.57	0.07
Coefficient of variation			0.107	0.069	0.045	0.123	0.036	0.323	0.143

Alloy: 2205
Transverse Compression (TC)

Specimen	t (mm)	l. rate ($N/mm^2/s$)	$s_{0.2}$ MPa	$s_{1.0}$ MPa	s_u MPa	elong. %	E_0 GPa	n	$s_{0.01}/s_{0.2}$
TC1	5	3	585.1	677.7			207.2	6.4	0.63
TC2	5	3	583.8	677.4			209.2	6.8	0.64
TC3	5	3	586.4	681.9			228.7	5.4	0.57
TC1	4.75	3	521.6	615.0			205.3	5.7	0.59
TC2	4.75	0.03	489.1	598.4			200.8	5.2	0.56
TC3	4.75	30	527.1	643.9			213.7	5.6	0.59
TC4	4.75	3	512.2	607.7			205.8	5.8	0.60
TC5	4.75	0.03	497.3	598.9			197.0	5.8	0.60
TC6	4.75	30	553.0	643.2			210.7	5.5	0.58
TC7	4.75	3	515.2	616.3			195.0	5.8	0.60
TC1	12	3	484.0	612.1			172.7	5.3	0.57
TC2	12	3	491.8	610.7			196.1	4.3	0.50
TC3	12	3	474.3	602.9			238.0	3.0	0.37
TC1	10	3	507.1	578.1			213.0	13.1	0.80
TC2	10	0.03	472.7	590.3			194.3	5.4	0.58
TC3	10	30	531.3	631.6			205.7	5.2	0.56
TC4	10	3	499.0	578.5			200.4	5.7	0.59
TC5	10	0.03	476.7	544.7			196.7	5.4	0.57
TC6	10	30	518.5	586.6			206.3	6.0	0.61
TC7	10	3	497.9	567.2			190.0	6.2	0.62
Average			516.2	613.2			204.3	5.9	0.6
Standard deviation			36.01	37.16			13.71	1.87	0.08
Coefficient of variation			0.070	0.061			0.067	0.318	0.129

Alloy: 2205
Longitudinal Compression (LC)

Specimen	t (mm)	l. rate ($N/mm^2/s$)	$s_{0.2}$ MPa	$s_{1.0}$ MPa	s_u MPa	elong. %	E_0 GPa	n	$s_{0.01}/s_{0.2}$
LC1	5	3	475.9	609.6			212.1	3.7	0.45
LC2	5	3	476.5	618.6			199.0	3.8	0.45
LC3	5	3	471.8	612.8			195.6	3.5	0.42
LC1	4.75	3	510.0	588.3			196.3	5.7	0.59
LC2	4.75	0.3	490.6	585.8			190.9	5.7	0.59
LC3	4.75	30	521.9	616.0			204.4	6.0	0.61
LC4	4.75	3	513.2	614.1			197.6	6.1	0.61
LC5	4.75	0.3	479.8	569.2			184.7	5.9	0.60
LC6	4.75	30	513.9	614.8			208.9	5.2	0.56
LC7	4.75	3	497.3	583.0			192.2	6.0	0.61
LC1	12	3	459.7	576.8			239.6	2.9	0.35
LC2	12	3	466.3	577.0			202.4	3.9	0.47
LC3	12	3	473.8	578.7			187.6	5.0	0.55
LC1	10	3	480.4	564.9			180.6	6.0	0.61
LC2	10	0.3	451.2	537.3			186.0	6.1	0.61
LC3	10	30	513.4	600.2			192.5	6.4	0.63
LC4	10	3	476.0	540.7			163.7	6.7	0.64
LC5	10	0.3	450.0	528.8			186.9	6.2	0.62
LC6	10	30	497.0	580.0			179.6	7.4	0.67
LC7	10	3	483.7	547.5			161.2	7.2	0.66
Average			485.1	582.2			193.1	5.5	0.6
Standard deviation			21.39	28.05			16.97	1.27	0.09
Coefficient of variation			0.044	0.048			0.088	0.232	0.156

Appendix B.2: South African Coupon Test Data

Test	Alloy[a]	Source[b]	Form[c]	E_0 GPa	$\sigma_{0.01}$ MPa	$\sigma_{0.2}$ MPa	σ_u MPa	ε_u	e	n	m[d]
20	430	7	P	195	209	304	518	0.29	0.0016	8.00	3.1
21	430	7	P	222	262	332	562	0.28	0.0015	12.5	3.1
22	430	7	P	196	219	331	517	0.30	0.0017	7.24	3.2
23	430	7	P	222	287	366	557	0.28	0.0016	12.4	3.3
24	430	7	P	195	235	312	510	0.30	0.0016	10.6	3.1
25	430	7	P	219	300	344	548	0.27	0.0016	22.0	3.2
26	430	7	P	195	235	334	521	0.23	0.0017	8.47	3.2
27	430	7	P	213	287	363	549	0.26	0.0017	12.8	3.3
28	3Cr12	8	P	196	222	318	480	0.30	0.0016	8.36	3.3
29	3Cr12	8	P	223	272	353	491	0.33	0.0016	11.4	3.5
30	3Cr12	8	P	201	236	307	482	0.27	0.0015	11.3	3.2
31	3Cr12	8	P	230	273	339	506	0.24	0.0014	13.9	3.3

a) UNS43000 ~ AISI430 ~ ENV1.4016, UNS41050 ~ 3Cr12 ~ ENV1.4003
b) 7 ~ van der Merwe & van den Berg (1987); 8 ~ van der Merwe et al. (1986)
c) P~ plate or sheet
d) The parameter *m* is obtained using Eqn. 17.